3-2020

Space-Based Localization of Radio Frequency Transmitters Utilizing Macaulay Resultant and Heuristic Optimization Methods

Jessica M. Wightman

Space-Based Localization of Radio Frequency Transmitters Utilizing Macaulay Resultant and Heuristic Optimization Methods

THESIS

Jessica Wightman, Captain, USAF

AFIT-ENY-MS-20-M-286

DEPARTMENT OF THE AIR FORCE
AIR UNIVERSITY

AIR FORCE INSTITUTE OF TECHNOLOGY

Wright-Patterson Air Force Base, Ohio

AFIT-ENY-MS-20-M-286

SPACE-BASED LOCALIZATION OF RADIO FREQUENCY TRANSMITTERS UTILIZING MACAULAY RESULTANT AND HEURISTIC OPTIMIZATION METHODS

THESIS

Presented to the Faculty

Department of Aeronautics and Astronautics

Graduate School of Engineering and Management

Air Force Institute of Technology

Air University

Air Education and Training Command

in Partial Fulfillment of the Requirements for the

Degree of Master of Science

Jessica Wightman, B.A., M.S.

Captain, USAF

March 2020

AFIT-ENY-MS-20-M-286

SPACE-BASED LOCALIZATION OF RADIO FREQUENCY TRANSMITTERS UTILIZING MACAULAY RESULTANT AND HEURISTIC OPTIMIZATION METHODS

Jessica Wightman, B.A., M.S.
Captain, USAF

Committee Membership:

Maj. Joshuah Hess, PhD
Chairman

Richard Cobb, PhD
Member

T. Alan Lovell, PhD
Member

Maj. Costantinos Zagaris, PhD
Member

Abstract

Space was once a rarely traveled domain but it is quickly becoming more accessible. More countries are developing space programs and more civilian companies are investing time and resources to exploring the reaches. When automobiles became accessible to the masses, roads had to be paved, traffic laws had to be written, and multiple local and national agencies stood up to monitor and enforce the domain. When airplanes became accessible, routes needed to be planned, traffic laws had to be written, and again multiple local and national agencies stood up to monitor and enforce the domain. The same is happening with the space domain. Space is becoming accessible enough to need planned trajectories, traffic laws, and an agency to monitor and enforce those safeguards. That agency will need all tools possible at their disposal to provide the best coverage and maintain space domain awareness, which requires accurate, timely, and precise knowledge of the tens of thousands of space objects.

This research focuses on radio frequency geolocation of space objects utilizing space-based platforms. Geolocation has long been the solution for locating objects. Technically, geolocation is the process of locating something on Earth (geo) but the term has been applied to all aspects of locating objects. In particular, this study examines the scenario of two cooperative receivers geolocating (or in this context, astrolocating) a transmitter in close proximity. A MATLAB algorithm is developed in this research to calculate the initial estimated transmitter location and projected orbital trajectory. The algorithm uses the Macaulay method of solving a system of polynomials as well as heuristic optimization techniques to locate a transmitter with respect to receivers at different time intervals. For the scenarios investigated, both

Macaulay and heuristic optimization methods achieve initial relative orbit determination for the transmitter.

Acknowledgements

Many thanks to my classmates. I would not have gotten this far without their support and motivation. Whether it was classwork or life, my classmates encouraged me every step of the way to do better and try harder.

Many thanks to my adviser, Joshuah Hess, for his enduring patience. I would not have survived my Master's time without your guidance and encouragement.

And finally, many thanks to my husband, Randal Direen, who supported me in this endeavor. He moved across the country with me. He held me when everything felt too hard. He dragged me along on hikes to clear my mind. And he pushes me every day to become a better version of myself. Love you, babe!

Jessica Wightman

Table of Contents

Page

List of Figures

List of Tables

List of Abbreviations

Abbreviation		Page
SDA	Space Domain Awareness	1
AFSPC	Air Force Space Command	1
USSF	United States Space Force	1
EM	Electromagnetic	2
IOD	Initial Orbit Determination	2
IROD	Initial Relative Orbit Determination	2
TDOA	Time Difference of Arrival	2
T	Transmitter	2
R1	Receiver One	2
R2	Receiver Two	2
RDOA	Range Difference of Arrival	2
LVLH	Local-Vertical, Local-Horizontal	3
HCW	Hill, Clohessy, Wiltshire	3
RSO	Resident Space Object	3
RF	Radio Frequency	3
ECI	Earth-Centered Inertial	6
NOAA	National Oceanic and Atmospheric Administration	8
NASA	National Aeronautics and Space Administration	8
GOES	Geostationary Operational Environmental Satellites	8
ESA	European Space Agency	8
GRACE	Gravity Recovery And Climate Experiment	8
NMC	Natural Motion Circumnavigation	8

Abbreviation		Page
ISS	International Space Station	9
HCW	Hill-Clohessy-Wiltshire	9
RAAN	Right Ascension of the Ascending Node	12
IOD	Initial Orbit Determination	13
IROD	Initial Relative Orbit Determination	13
POD	Precise Orbit Determination	13
LEO	Low Earth Orbit	14
GEO	Geosynchronous Orbit	14
TDOA	Time Difference of Arrival	15
TOA	Time of Arrival	16
FDOA	Frequency Difference of Arrival	16
PSO	Particle Swarm Optimization	20
STM	State Transition Matrix	23

SPACE-BASED LOCALIZATION OF RADIO FREQUENCY TRANSMITTERS UTILIZING MACAULAY RESULTANT AND HEURISTIC OPTIMIZATION METHODS

I. Introduction

1.1 Motivation

Space domain awareness (SDA) or the identification, characterization and understanding of any factor that could affect space operations [1] has traditionally fallen on Air Force Space Command (AFSPC). The newly created United States Space Force (USSF) will now take lead on this task [2]. Just as the US Air Force was tasked at its creation with maintaining air superiority the USSF is tasked with maintaining space superiority [2]. And space superiority involves knowing what objects are present in the domain and where they are or can be located.

More than 2000 operational satellites orbit the Earth today [3]. New satellites are being launched every month. SpaceX has started launching a constellation called Starlink consisting of over 1000 small satellites to provide worldwide internet [4]. This increases orbiting operational satellites by fifty percent. But operational satellites are not the only concern. Orbital debris such as rocket bodies, decommissioned satellites and broken satellite parts make up the majority of the space threats. There are more than 20,000 pieces of orbital debris larger than a softball [5]. And it is estimated that there are more than 500,000 pieces of space debris larger than a marble [5]. With the debris travelling at speeds up to 17,500 miles per hour, every piece of debris could potentially become a lethal threat to an operational satellite. To maintain accurate

and reliable SDA, the USSF needs to utilize any and all methods for localization.

Localization involves using some form of sensor along with a processing technique to locate another object. Localization sensors collect data in all ranges of the electromagnetic (EM) spectrum [6]. Signal measurements can be taken with respect to time, frequency, direction, strength, or any combination of these. Geolocation focuses on estimating the position of an object. In space, the position is only half the battle. The object's state vector, comprised of the position and the velocity of the object, tells the story of where the object came from and where it is headed. For a satellite, the positions and velocity can be defined as an initial orbit determination (IOD) or initial relative orbit determination (IROD) problem. This research defines satellite localization as astrolocation.

1.2 Methodology

This research will approach the localization problem by examining the time a signal arrives at a pair of satellite receivers. More specifically, the time difference of arrival (TDOA) between the transmitter (T) signal arriving at receiver one (R1) versus arriving at receiver two (R2) will be utilized to evaluate the range difference of arrival (RDOA). The RDOA equation expands to a multivariate polynomial in terms of both receiver locations as well as the transmitter location at specific times. A resultant multivariate polynomial solver called the Macaulay Resultant will be examined as an option to solve for the initial state vector and IROD of the transmitter. The Macaulay solver will be compared to a heuristic optimization solver to evaluate its effectiveness. A MATLAB® simulation will be developed to analyze the polynomial solvers, different receiver formation geometries and how well those receiver geometries solve the astrolocation problem, as well as analyze the geometry between the receivers and the transmitter including orbital regime.

1.3 Underlying Assumptions

Scenarios will be defined in the local-vertical, local-horizontal (LVLH) frame. The chief of the LVLH frame is assumed to have a circular inertial orbit. A circular chief orbit and calculations done in the LVLH frame allow for the dynamics to be treated as linear and the Hill, Clohessy, Wiltshire (HCW) model used [7]. The scenarios will ignore the effects of J2 and higher perturbations. Relativistic effects are not considered, i.e. the speed of light is constant, inferring $(TDOA)c = RDOA$. Also, the accuracy of clock timing is not addressed. It is assumed that the receiver states are known with zero uncertainty. It is assumed that the signal processing for the TDOA measurement is accomplished before the process examined in this research begins. Due to the complexities of the Macaulay resultant theory, the algorithm assumes coplanar motion between R1, R2 and T; however, cross-track motion is allowed for the heuristic optimization method.

1.4 Research Objective

The objective of this research is to develop an algorithm to enhance space-based SDA. The specific capability to be advanced is the relative orbit determination of resident space objects (RSO) given radio frequency (RF) data from space-based observers. Multiple relative geometries of the receivers as well as multiple relative trajectories of the transmitter will be explored. By taking measurements at several time steps, an RDOA measurement history can be found, setting up a system of polynomials.

This research also aims to draw conclusions about astrolocation in general by asking the following questions:

- Given two cooperative receivers, what formation geometries are effective or ineffective at astrolocating a transmitter?

- Given a formation geometry for two cooperative receivers, what are potential transmitter geometries for which IROD is possible?
- And given a geometry between receivers and a transmitter, how does the orbital regime influence the IROD solution?

The Macaulay resultant method presents a way to solve the system of polynomials to find the IROD. Due to an initial survey of the Macaulay resultant method showing little evidence of the Macaulay method being used for IROD, Heuristic optimization methods are used in parallel with the Macaulay method to ensure research objective accomplishment.

1.5 Thesis Organization

This thesis is organized into five chapters. First, Chapter I addresses the problem and its motivation. Chapter II discusses existing geolocation techniques, relative satellite motion, and orbit determination. Chapter III outlines the process behind the developed algorithm. Chapter IV explores the results of specific scenarios using the algorithm. Chapter V concludes the research with summarized results and contributions along with recommendations for future research.

II. Background

2.1 Overview

This research develops an algorithm to determine the initial relative orbit of a satellite emitter using a formation of cooperative receiver satellites. The process of locating an object and determining its orbit can take many forms. Figure 1 shows a sampling of options one can explore to develop a localization algorithm. The parameters highlighted in yellow depict what is used for this research.

Figure 1. Localization Parameters

This chapter addresses the definitions of these parameters as well as explores some research that has already been accomplished with respect to these parameters.

2.2 Orbital Motion

Johannes Kepler is credited with the laws of planetary motion. First, the planets are in elliptical orbits around the sun with the sun at one focus of the ellipse. Sec-

ond, the position/radius vector of the orbit sweeps through equal areas of the ellipse in equal times. And, third, the period of the orbit squared is proportional to the semimajor axis cubed [8].

The combination of Newton and Kepler's work is where satellite motion begins. Orbital motion of satellites can be reduced to a two-body gravitational problem [8]. Due to proximity, the strongest gravitational force on a satellite is from the Earth, and gravitational forces from the Sun, the moon and other planets are treated as negligible.

2.2.1 Reference Frames.

Before specific orbits can be characterized, reference frames need to be defined. The Earth-centered inertial (ECI) frame originates from the center of the Earth. Seen in Figure 2, the **i** vector is in the direction of the vernal equinox. The **k** vector is vertical through the north pole, and the **j** vector completes the right-handed triad, lying in the equatorial plane pointing orthogonally eastward from the **i** direction.

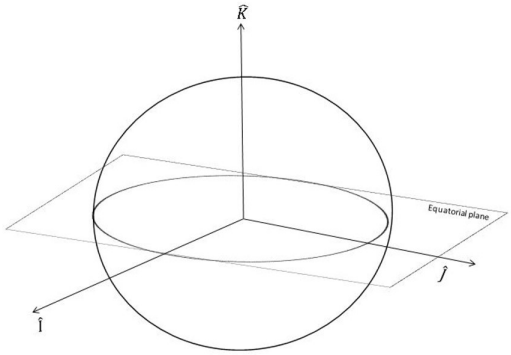

Figure 2. Earth-Centered Inertial Reference Frame [9]

This research uses the ECI frame as reference for the inertial orbit definition. However, calculations for the TDOA/IROD problem are in the local-vertical, local

horizontal (LVLH) frame.

With two satellites in close proximity, the relative orbital dynamics can be approximated by linear differential equations and visualized in the LVLH frame. The origin of the LVLH frame can be a satellite (sometimes called the chief) or simply a point in a reference orbit. The rotating LVLH frame moves with the chief's orbit around the Earth. Seen in Figure 3, the **X** vector defines the radial direction of the frame. The **Z** vector is parallel to the chief's orbital angular momentum vector in the orbit normal direction. The **Y** vector completes the right-handed triad perpendicular to **X** and points in the general direction of the orbit track. In the LVLH frame, **X**, **Y**, and **Z** are referred to as the radial, in-track, and cross-track directions, respectively.

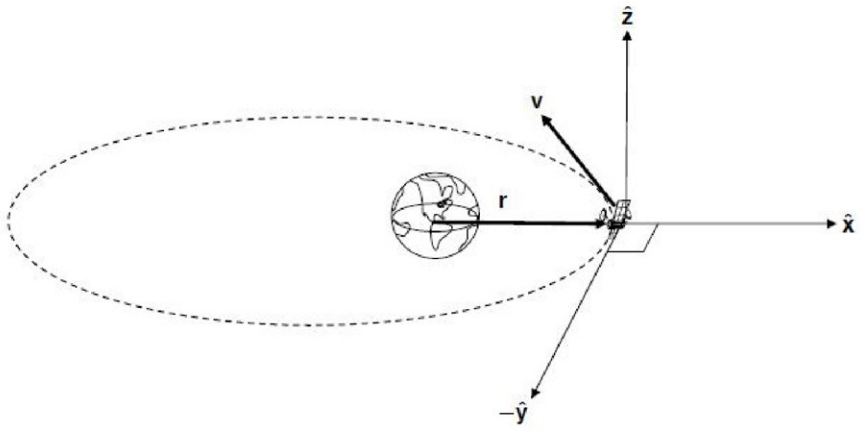

Figure 3. Local-Vertical, Local-Horizontal Reference Frame [10]

2.2.2 Formation Flying.

The maintenance of a desired relative separation, orientation, or position between or among spacecraft is called formation flying [11]. This is simply multiple satellites

working collaboratively by maintaining a specific flying geometry. The relative motion between the formation is chosen based on the mission.

One type of formation is called a constellation. This is a global-scale group of satellites working together. GPS satellites are arranged with at least six satellites in six orbital planes around the world, so that at any one point in time, there are at least three satellites in view of any position on Earth [12]. Local ground topography such as hills and buildings might obscure this view, but the satellites are there. Another constellation mission is performed by the National Oceanic and Atmospheric Administration (NOAA) and the National Aeronautics and Space Administration (NASA) using the Geostationary Operational Environmental Satellites (GOES) satellites [13]. There are two GOES satellites covering all land inside US borders. The satellites provide advanced imaging for accurate forecasts, real-time mapping of lightning activity, and monitoring of solar activity and space weather.

Another type of formation is called a leader/follower formation. Satellites in this formation are at the same radial distance from ECI, but they are offset by some value in the in-track direction of the orbital plane. This formation can be centered on an LVLH frame, or can be spread out through a full orbital plane surrounding the Earth. The GOES constellation could also be considered a leader/follower formation. Another mission in a leader/follower formation is the European Space Agency (ESA) Gravity Recovery And Climate Experiment (GRACE) mission. GRACE uses the relative distance between two satellites in the LVLH frame to measure Earth's gravity field over time [14].

Another formation is called natural motion circumnavigation (NMC). In this formation, a satellite maintains a specific velocity that allows the satellite to circumnavigate around a point in the LVLH frame. The velocity is also an energy matching condition between the chief and the deputy. The point at the center of the ellipse

may be located at the origin of the LVLH frame or could be offset from the origin. It is often suggested that the International Space Station (ISS) could utilize inspector satellites in NMCs around the ISS to assess the structure for external damage. This technique has yet to be employed by the ISS, citing unintended damage and risk as the reasons to forego the practice [15].

Figure 4 shows an example of how one satellite might move in relation to the other. The chief is at the center of the LVLH reference frame and the deputy's motion is related to the chief by the relative position vector ρ. The way this motion propagates as the satellites orbit Earth will determine the relative orbital dynamics (NMC or leader/follower).

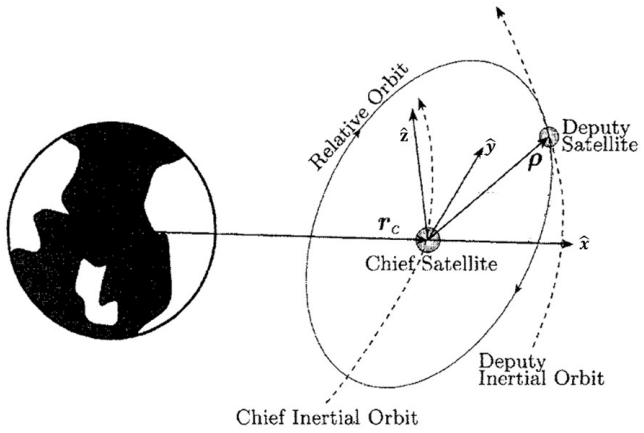

Figure 4. Notional Relative Orbit [16]

Clohessy and Wiltshire [7] built on the work of Hill looking at a chief in a near circular inertial orbit around earth to solve the equations of motion for a deputy in a relative orbit around a chief at close proximity. These are referred to as Hill-Clohessy-Wiltshire (HCW) equations of motion and are shown in Equation 2.1.

$$\begin{aligned} \ddot{x} - 3n^2x - 2n\dot{y} &= 0 \\ \ddot{y} + 2n\dot{x} &= 0 \\ \ddot{z} + n^2z &= 0 \end{aligned} \tag{2.1}$$

where x, y, and z are the radial, in-track and cross-track relative positions of the deputy with respect to the chief in the LVLH frame and n is the mean motion of the chief's inertial orbit. Figure 5 depicts this relative position as component vectors.

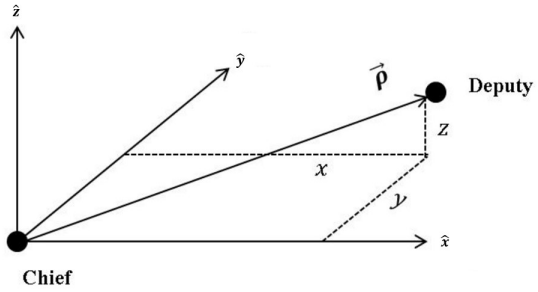

Figure 5. Deputy Position Relative to Chief [9]

There are many other relative dynamics models that have been developed. Each one takes into account slightly different parameters, such as chief orbit eccentricity or perturbation effects. The major assumption of the HCW model is that the chief is in a near-circular orbit around the earth [7]. Other models might allow for more chief orbit eccentricity or they might take into account types of perturbations that could affect the chief orbit. As a feasibility study, this research starts with the HCW model.

The relative motion relationships in the LVLH frame can be used to describe the motion of a formation of satellites, i.e. between the two receiver satellites in the

TDOA/IROD problem presented in this research. But, relative motion can also be used to describe the motion of another satellite or object in relation to the formation, i.e. the motion of the transmitter around the receivers. This research will explore the use of these dynamics for localization.

Researchers Cajacob et. al [17] found that the farther apart the receiver satellites are, the more accurate the localization measurement is. However, the idea of HCW relative motion is that the objects are close to each other. The research presented here will look at the specific geometries of a formation of receiver satellites that will be able to perform a localization mission despite the 'close' relative separation.

2.2.3 Orbit Determination.

Orbit determination is the process of taking observed data about a satellite's position and defining the satellite state vector (position and velocity) in 3-dimensional space or defining a set of orbital parameters (orbital elements). These orbital elements define the trajectory an object will follow over time. Orbit determination can be done in the ECI frame to get an inertial orbit or in the LVLH frame to get a relative orbit. Figure 6 shows how an orbit is defined with the classical orbital elements.

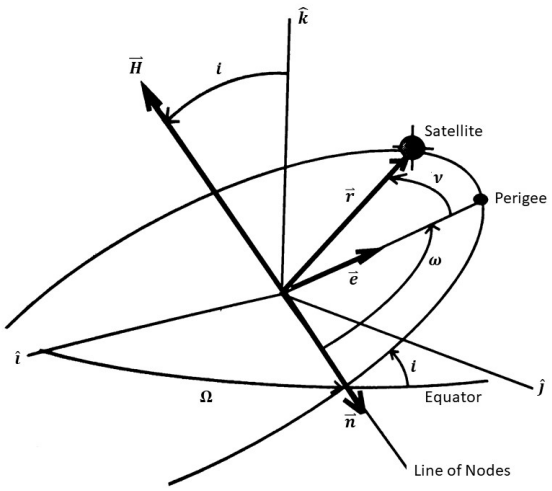

Figure 6. Orbit Parameters [8]

The trajectory of the orbit is located at a radius r from the central body that is located at the focal point of the ellipse. The eccentricity of the orbit is defined by parameter e. Inclination, i, is the angle between the orbital plane and the equatorial plane. The Right Ascension of the Ascending Node (RAAN), indicated by Ω, is the angle from $\hat{i}$ (vernal equinox) to the ascending node of the orbit (the point at which the trajectory crosses the equatorial plane). The argument of perigee, ω, is the angle from the ascending node to the direction of perigee (the point of the ellipse closest to the occupied focus). True anomaly, ν, is the angle from perigee to the radial location vector. Figure 7 shows the final parameter that is needed to define an orbit. The semi-major axis, a, is half the distance from apogee to perigee. Other parameters of the orbit include the distance from the focus to the orbit trajectory, p, and the semi-minor axis, b.

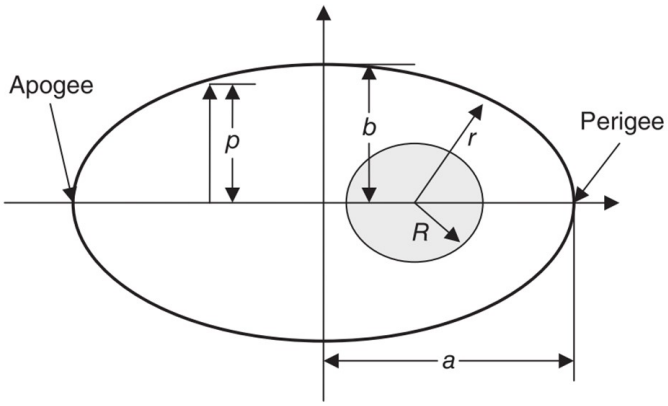

Figure 7. Elliptical Orbit Shape Parameters [18]

The six classical orbit elements are defined by

$$[\text{œ}] = [a \quad e \quad i \quad \Omega \quad \omega \quad \nu]^T \tag{2.2}$$

Each of the orbit elements can be calculated from the position and velocity vectors of the satellite at different times throughout the trajectory [19]. Multiple observations of the satellite's motion are needed to calculate an accurate orbit trajectory.

Orbit determination is defined in terms of fidelity. Initial orbit determination (IOD) and initial relative orbit determination (IROD) both take the measurements of the satellite motion and determine a coarse initial estimate for the orbital motion [8, 20]. IOD is with respect to the inertial frame. And IROD is with respect to the relative, LVLH, frame. Precise orbit determination (POD) requires an initial estimate of the orbit dynamics (IOD or IROD) and then refines that estimate into a more accurate and precise orbit definition.

This research will focus on the use of RF data to calculate position, velocity and

orbit data. This research will not explore the signal processing when a measurement is taken, but rather the IROD process after the measurements are received. The development of this algorithm will use the signal's time difference of arrival. The receivers will be in a formation in either Low Earth Orbit (LEO) or GEO-synchronous Orbit (GEO), and the emitter will be in close enough proximity for HCW dynamics to remain valid. This research will focus on relative motion of the objects.

2.3 Localization

Localization is the process of locating an object. In general, a point can be located in 3-dimensional space with the intersection of three or more vectors or planes [18]. Localization can be done with one receiver or many. Localization can be accomplished using any frequency in the EM spectrum depending on what sensors are on the receiver and where those receivers are located [6]. This research will focus on the RF portion of the EM spectrum.

By using several locator receivers, intersections can be found at one measurement time for possible location solutions [21]. If the emitting frequency is unknown, the locator must do some other analysis to gain understanding about the source. Data can be processed in different ways to gain insight into the location of the source. Directionality, time, and phase are common ways to look at incoming signals. The following sections will explore the different types of signal measurements used for localization.

2.4 Signal Measurement and Processing

Once the location of the receivers is known, the process of localization of a transmitter can begin. Localization can be divided into two steps, measurement and estimation. The measurement step utilizes a specific type of data based on the sen-

sor of the receiver. This research will use the signal's time of arrival to accomplish astrolocation.

2.4.1 Time Difference of Arrival.

Time difference of arrival (TDOA) is the characterization of a signal based on the different times that it arrives at multiple receivers. For geolocation in 3-Dimensional space, at least three sets of unrelated TDOA measurements are needed [18].

At the time of measurement, the inertial location of three receiver satellites and an emitter are $O_0(x_0, y_0, z_0)$, $O_1(x_1, y_1, z_1)$, $O_2(x_2, y_2, z_2)$, and $T(x, y, z)$, as shown in Figure 8.

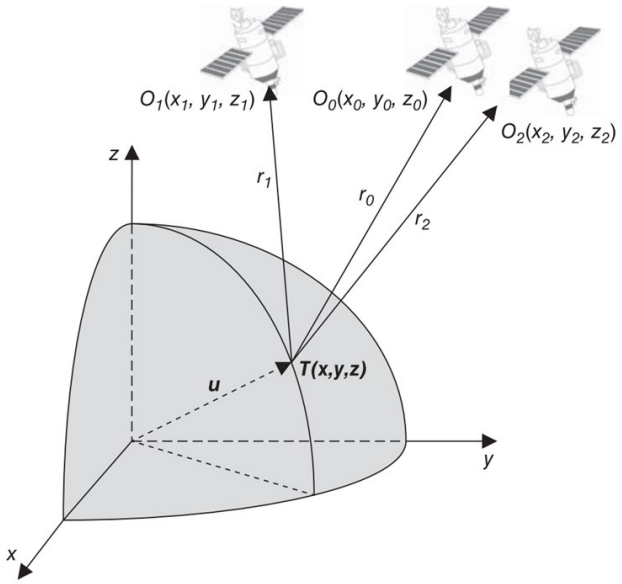

Figure 8. TDOA Geolocation [18]

The distance from emitter to receiver r_i in Figure 8 is defined as:

$$r_i = \sqrt{(x - x_i)^2 + (y - y_i)^2 + (z - z_i)^2} \tag{2.3}$$

where $x,\ y,$ and z are the location of the transmitter.

Two unique TDOAs can be found using time of arrival (TOA) from three satellites.

$$TDOA_i = TOA_i - TOA_0 = \Delta t_i \tag{2.4}$$

Recall, localization requires three sets of unrelated data [10]. For this example, there are two TDOA measurements. The third data point is typically the surface of the earth [10].

Electromagnetic waves (and RF signals) travel at the speed of light, c. Using the TDOAs, the difference in distance to each of the receivers can be found.

$$r_i - r_0 = \Delta r_i = c\Delta t_i \tag{2.5}$$

By substituting the ranges from Equation (2.3) into Equation (2.5), and determining where these surfaces intersect the surface of the Earth, the inertial position $T(x, y, z)$ is determined.

2.4.2 Frequency Difference of Arrival.

Frequency Difference of Arrival (FDOA) uses the difference in measured frequency at the receiver to gain information about the source [10]. Because the receivers and emitter are moving, the observed and measured frequency is actually the Doppler shifted frequency. The change in Doppler frequency from receiver to receiver is given by Equation (2.6).

$$\Delta f_d = -f_0 \Delta \dot{t} \tag{2.6}$$

where f_0 is the frequency of the signal from the emitter.

$\Delta \dot{t}$ can be found by differentiating Equation (2.5).

$$\dot{r}_i - \dot{r}_0 = \Delta\dot{r}_i = c\Delta\dot{t}_i \tag{2.7}$$

Putting Equations (2.6) and (2.7) together, one finds

$$\Delta\dot{r} = -\frac{c}{f_0}\Delta f_d \tag{2.8}$$

Equation (2.8) is the FDOA equation. Similar to TDOA, three unrelated FDOA equations are needed to locate an emitter.

2.4.3 Hybrid Models.

Combining methods of measurement can help decrease the number of data points needed or the number of receivers needed at a given measurement time. For example, Figure 9 shows how two satellites can be used to geolocate an object using TDOA, FDOA, and the surface of the Earth as the intersecting vectors [10].

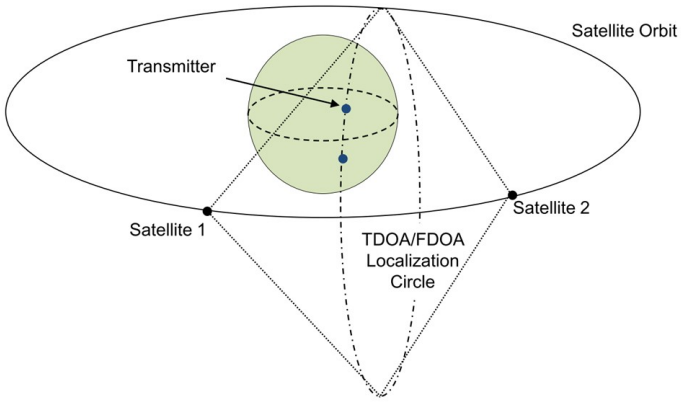

Figure 9. Hybrid Geolocation [10]

With TDOA or FDOA alone, four receivers are needed for the three independent range vectors [18]. By combining methods, only three vectors (from three receivers

or two receivers and the surface of the earth) are needed at a given time to locate the instantaneous position of an object.

Another way to reduce the number of receivers is to increase the number of observations [10]. Each of the models explored above look at determining the instantaneous position of an object using one observation window. Figure 10 depicts the concept of multiple time observations of a moving receiver with a stationary transmitter.

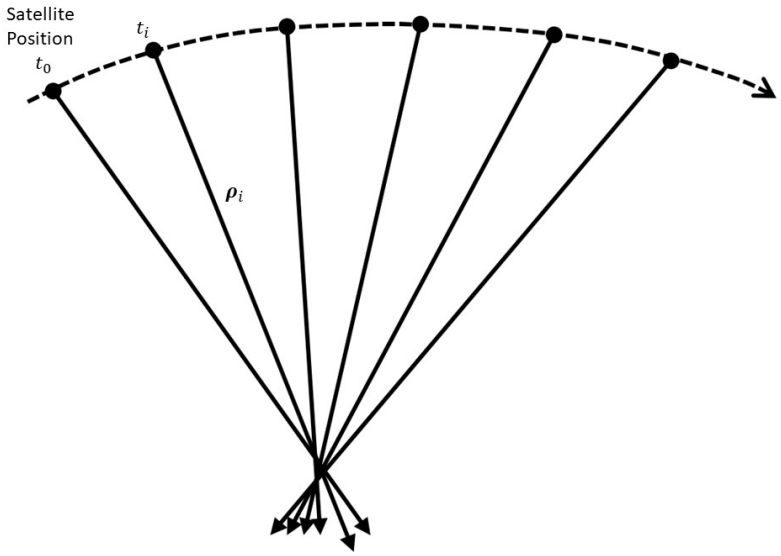

Figure 10. Single Satellite Geolocation [10]

Single satellite geolocation is more accurate with the more data points that can be measured [10]. But, single platform geolocation is most effective on a stationary emitter. Bailey [21] wrote his master's thesis focusing around single platform geolocation. Sinclair et al. [22] explore the accuracy of heterogeneous TDOA or taking measurements at multiple locations. Shuster et al. [23] expand on the Sinclair et al. work to explore the accuracy of heterogeneous TDOA IROD. The research presented here will have a moving emitter where multiple observations will correspond to different points in the emitter's orbit trajectory.

2.5 Solving Methods

The problem of locating a moving object has many different ways to solve it [18]. On one extreme, one could use many receiver satellites, all looking for the same object at one time. The other extreme uses one receiver watching over a long period of time to map out the transmitter's trajectory. This research will explore in between these extremes with multiple satellites taking measurements at multiple times. A system of polynomials will be formed with the measurement data.

2.5.1 Resultant Methods and Macaulay.

The resultant of a set of multivariate polynomials is a single univariate polynomial obtained by eliminating all of the other variables [24]. For example, if the equations that are to be solved are functions of $x_1,\ x_2,\ x_3,\ \ldots\ x_n$, then by eliminating the variables $x_2,\ \ldots\ x_n$, the resultant is given by $R(x_1)$. Macaulay uses the coefficients of the original polynomials to form the resultant [25, 26].

The Macaulay resultant method consists of three main steps: constructing a matrix polynomial in terms of an anchor variable, computing the anchor variable, and solving for the remaining roots or variables [24].

Consider the system of n polynomial equations with n unknowns as shown in Equation (2.9). The degrees of the equations are $d_1,\ d_2,\ \ldots,\ d_n$.

$$\begin{aligned} F_1(x_1,\ x_2,\ \ldots,\ x_n) &= 0 \\ F_2(x_1,\ x_2,\ \ldots,\ x_n) &= 0 \\ &\ldots \\ F_n(x_1,\ x_2,\ \ldots,\ x_n) &= 0 \end{aligned} \tag{2.9}$$

Resultants can be used to eliminate all except an anchor variable. A resultant is a polynomial comprised of the coefficients of the original system. The Macaulay

method also expresses the resultant as a ratio of determinants of two matrices **M** and **D**, seen in Equation (2.10).

$$R(x_1) = \frac{det(M)}{det(D)} \tag{2.10}$$

where **M** and **D** are matrix polynomials in terms of the original system coefficients and the anchor variable, x_1. If **D** is non singular, the roots of **M** correspond to the roots of x_1 in the original system. In this way, solving for the anchor variable becomes an eigenvalue problem where

$$M(x_1)(1,\ x_2,\ \ldots,\ x_n,\ \ldots,\ {x_2}^d,\ {x_3}^d,\ \ldots,\ {x_n}^d)^T = (0,\ 0,\ \ldots,\ 0,\ \ldots,\ 0,\ 0,\ \ldots,\ 0)^T \tag{2.11}$$

Once the anchor variable is known, the remaining roots simply correspond to the kernel of $\mathbf{M}(x_1)$. This process will be discussed in greater detail in Chapter III. Legrand et. al [24] built on the work of Morgan [26] and Manocha [25] to use the Macaulay method to solve a system of polynomials. The research presented here will explore the use of Macaulay to solve a TDOA IROD problem.

2.5.2 Heuristic Optimization and PSO.

Heuristic optimization is a form of stochastic optimization where a degree of randomness is introduced and used to find some an optimal solution [27]. The heuristic process presented in this research is the Particle Swarm Optimization (PSO) algorithm.

PSO mimics the motion of a flock of birds. The motion appears random to the observer but the swarm, as a whole, has an objective. To solve any problem, a specific objective, or cost function, is selected. Then an initial swarm of random particles is distributed throughout the solution space. These particles are possible

solutions that minimize the cost function. Next, solver settings are chosen. These settings include the bounds for the solution space, the tolerance for a solution, the swarm size in terms of particles, the number of iterations to search for the solution, and a processing algorithm.

Throughout iterations, the particle's receive updates in three ways. First is an inertial update. This updates the particle proportionally with respect to the cost function. For example, localization of an RSO is based on the satellite position and velocity. For the inertial update, the PSO solver takes the difference of position and velocity of the previous update into account for the current position and velocity update.

For the next update, a particle receives a cognitive update. This is an update confirming a certain particle's motion and that it is headed in the right direction toward a likely solution based on what that specific particle can sense. The third update, a social update, goes to particles that are headed in the right direction according to the swarm as a whole. Again, the measure for 'right direction' is the cost function and the tolerance to which a solution is desired. The particles continue to receive updates up to the iteration threshold or until the solution is within the cost function tolerance.

PSO is widely used due to its robustness [28]. Riccardo Poli [28] published a survey on the uses of PSO ranging from antenna design and communication networks to biomedical, financial and scheduling. Poli demonstrated that with PSO any cost function can be input and any solution found within a tolerance. Lujan et. al [29] utilized the PSO method to determine optimal receiver formation geometries for space-based TDOA localization. The research presented here will expand the Lujan research to look at receiver formations geometries for TDOA IROD.

2.6 Summary

Chapter II has discussed existing geolocation techniques, relative satellite motion, and orbit determination. Chapter III outlines the process behind the algorithm developed as part of this research.

III. Methodology

3.1 Overview

As seen in Section 2.4.1, with TDOA, only the time the signal arrives at the receiver is necessary to locate the object. An alternative form of TDOA is found by examining the relative distance the signal travels from the transmitter to two different receivers.

$$\begin{aligned} RDOA &= c\ (TDOA) \\ RDOA(t_i) = \rho(t_i) &= \sqrt{\mathbf{X}_T(t_i) - \mathbf{X}_{R1}(t_i)} - \sqrt{\mathbf{X}_T(t_i) - \mathbf{X}_{R2}(t_i)} \end{aligned} \tag{3.1}$$

where $\mathbf{X}_T$, $\mathbf{X}_{R1}$, and $\mathbf{X}_{R2}$ are the state vectors of the transmitter, receiver one, and receiver two, respectively. t_i is the time the measurement is taken.

The position of the transmitter in Equation (3.1) is the position in reference to a specific measurement time. Taking multiple measurements sets up a system of polynomials to solve for the position of the unknown transmitter. At least one measurement per number of unknowns is needed to solve the localization problem.

3.2 The System of Equations

Space objects are free to move in 3-dimensions. Those objects have an instantaneous position vector, $[x,\ y,\ z]^T$ and velocity vector, $[\dot{x},\ \dot{y},\ \dot{z}]^T$ with respect to the LVLH frame. Given an initial state vector, the states at any other point in time can be found using a State Transition Matrix (STM), $\mathbf{\Phi}(t, t_0)$, such that

$$\mathbf{X}(t) = \mathbf{\Phi}(t, t_0)\mathbf{X}(t_0) \tag{3.2}$$

For this research, HCW dynamics will be used. Therefore,

$$\mathbf{\Phi}_{HCW} = \begin{bmatrix} 4-3\cos nt & 0 & 0 & \frac{1}{n}\sin nt & -\frac{2}{n}(\cos nt-1) & 0 \\ 6\sin nt-6nt & 1 & 0 & \frac{2}{n}(\cos nt-1) & \frac{1}{n}(4\sin nt-3nt) & 0 \\ 0 & 0 & \cos nt & 0 & 0 & \frac{1}{n}\sin nt \\ 3n\sin nt & 0 & 0 & \cos nt & 2\sin nt & 0 \\ 6n(\cos nt-1) & 0 & 0 & -2\sin nt & 4\cos nt-3 & 0 \\ 0 & 0 & -n\sin nt & 0 & 0 & \cos nt \end{bmatrix} \tag{3.3}$$

To solve for the position of the transmitter in the RDOA equation, only the top half of the STM is needed,

$$\begin{bmatrix} x(t) \\ y(t) \\ z(t) \end{bmatrix} = \begin{bmatrix} 4-3\cos nt & 0 & 0 & \frac{1}{n}\sin nt & -\frac{2}{n}(\cos nt-1) & 0 \\ 6\sin nt-6nt & 1 & 0 & \frac{2}{n}(\cos nt-1) & \frac{1}{n}(4\sin nt-3nt) & 0 \\ 0 & 0 & \cos nt & 0 & 0 & \frac{1}{n}\sin nt \end{bmatrix} \begin{bmatrix} x(t_0) \\ y(t_0) \\ z(t_0) \\ \dot{x}(t_0) \\ \dot{y}(t_0) \\ \dot{z}(t_0) \end{bmatrix} \tag{3.4}$$

Equation (3.4) is substituted into the RDOA equations so that each equation is no longer in terms of position at each time, but in terms of the initial state of the transmitter. Now, there is a system of equations in terms of a common six unknowns. In general, a polynomial with six unknowns ($x,\ y,\ z,\ \dot{x},\ \dot{y},\ \dot{z}$) is given by Equation 3.5.

$$
\begin{aligned}
f_1(x,\ y,\ z,\ \dot{x},\ \dot{y},\ \dot{z}) = {} & a_1x^2 + a_2xy + a_3xz + a_4x\dot{x} + a_5x\dot{y} + a_6x\dot{z} + a_7x + \\
& a_8y^2 + a_9yz + a_{10}y\dot{x} + a_{11}y\dot{y} + a_{12}y\dot{z} + a_{13}y + \\
& a_{14}z^2 + a_{15}z\dot{x} + a_{16}z\dot{y} + a_{17}z\dot{z} + a_{18}z + \\
& a_{19}\dot{x}^2 + a_{20}\dot{x}\dot{y} + a_{21}\dot{x}\dot{z} + a_{22}\dot{x} + \\
& a_{23}\dot{y}^2 + a_{24}\dot{y}\dot{z} + a_{25}\dot{y} + \\
& a_{26}\dot{z}^2 + a_{27}\dot{z} + a_{28} = 0
\end{aligned}
\tag{3.5}
$$

where, for this research, the coefficients encompass the known data about R1 and R2 and $[x,\ y,\ z,\ \dot{x},\ \dot{y},\ \dot{z}]^T$ is the state vector of the transmitter at t_0.

This research ignores the effects of J_2, assumes linear dynamics within the LVLH frame (HCW dynamics), and assumes co-planar motion (i.e. z and $\dot{z} = 0$). Therefore, the scenario will start with four equations and four unknowns at four different receiver times. For co-planar motion, the generic equation becomes

$$
\begin{aligned}
f_1(x\ \ y\ \ \dot{x}\ \ \dot{y}) = {} & a_1x^2 + a_2xy + a_3x\dot{x} + a_4x\dot{y} + a_5x + \\
& a_6y^2 + a_7y\dot{x} + a_8y\dot{y} + a_9y + \\
& a_{10}\dot{x}^2 + a_{11}\dot{x}\dot{y} + +a_{12}\dot{x} + \\
& a_{13}\dot{y}^2 + a_{14}\dot{y} + a_{15} = 0
\end{aligned}
\tag{3.6}
$$

3.3 Application of Macaulay

To use the Macaulay resultant method, the system of equations must first be rewritten in terms of an anchor variable (any of the variables in the system can be anchor variables). For this research, $\dot{y}$ will be the anchor variable and for setup,

treated as a constant.

$$\begin{aligned} f_1(x,y,\dot{x},\dot{y}) = a_1x^2 + a_2xy + a_3x\dot{x} + (a_4\dot{y} + a_5)x + a_6y^2 + \\ a_7y\dot{x} + (a_8\dot{y} + a_9)y + a_{10}\dot{x}^2 + (a_{11}\dot{y} + a_{12})\dot{x} + \\ (a_{13}\dot{y}^2 + a_{14}\dot{y} + a_{15}) = 0 \end{aligned} \tag{3.7}$$

3.3.1 Homogenization.

In order to form the Macaulay matrix polynomial equation, the original polynomial equations need to be homogeneous. Homogeneity requires the degree of all monomials within each polynomial to be equal. This is accomplished by adding a homogenization variable w.

$$\begin{aligned} f_1(x,y,\dot{x},w) = A_1x^2 + A_2xy + A_3x\dot{x} + A_4xw + A_5y^2 + A_6y\dot{x} + \\ A_7yw + A_8\dot{x}^2 + A_9\dot{x}w + A_{10}w^2 = 0 \end{aligned} \tag{3.8}$$

where

$$\begin{aligned} &A_1 = a_1, \quad A_2 = a_2, \quad A_3 = a_3, \quad A_4 = a_4\dot{y} + a_5, \\ &A_5 = a_6, \quad A_6 = a_7, \quad A_7 = a_8\dot{y} + a_9, \\ &A_8 = a_{10}, \quad A_9 = a_{11}\dot{y} + a_{12}, \quad A_{10} = a_{13}\dot{y}^2 + a_{14}\dot{y} + a_{15} \end{aligned} \tag{3.9}$$

3.3.2 Matrix Size.

Before the Macaulay matrix polynomial equation can be formed, the resultant matrix $\mathbf{M}$ needs to be constructed. The size of $\mathbf{M}$ is based on the total degree of the set of polynomials, D, the number of variables (not including the homogenization variable), n, and the number of equations, m. The total degree D of the set of polynomials is computed as

$$D = 1 + \sum_{i=1}^{m}(d_i - 1) \tag{3.10}$$

where d_i is the degree of the i^{th} equation.

The size of $\mathbf{M}$ is directly related to the system's total degree and number of variables.

$$size\ (\mathbf{M}) = \begin{pmatrix} (n-1)+d \\ (n-1) \end{pmatrix} \tag{3.11}$$

For this research, $n = 4$ and all polynomials are of degree 2, so the total degree of the system is

$$D = 1 + (d_1 - 1) + (d_2 - 1) + (d_3 - 1) + (d_4 - 1) = 5$$

and

$$\text{size } (\mathbf{M}) = \begin{pmatrix} 3 & + & 5 \\ & 3 & \end{pmatrix} = 56$$

This means that $\mathbf{M}$ is a 56 x 56 matrix.

The $\mathbf{M}$ matrix is formed out of the coefficients of Equation (3.8). However, to determine coefficient placement, column and row labels are needed for reference.

3.3.3 Column and Row Labels.

The columns of $\mathbf{M}$ correspond to all monomials up to the degree of the system. All monomial exponents add up to the degree of the system. For this research, the system degree is $d = 5$. From left to right, the monomials are arranged in lexicographical order as seen in Equation (3.12).

$$\mathbf{M} = \begin{array}{c|cccccccccc} & x^5 & x^4y & \ldots & xw^4 & y^5 & y^4\dot{x} & \ldots & \dot{y}w^4 & w^5 \\ \hline & & & & & & & & & \end{array} \tag{3.12}$$

The rows of $\mathbf{M}$ come from the corresponding equation of the column big (marker) variable multiplied by the same numbered row monomial and divided by the marker

variable squared [24].

'Big' refers to the exponent of the variable. For example, in Equation (3.12), the first column big variable is x. In the last two columns, the big variable is w. For any monomial where the exponents are tied, the left variable with the big exponent is the marker variable. For example, for monomial $xy^2\dot{x}^2$, y is the marker variable [24].

The 'corresponding equation' comes from numbering the variables. If the variables in the coefficients are numbered as a state vector,

$$\begin{bmatrix} x \\ y \\ \dot{x} \\ w \end{bmatrix} = \begin{bmatrix} 1 \\ 2 \\ 3 \\ 4 \end{bmatrix} \tag{3.13}$$

then if x is the marker variable, the corresponding equation is f_1. If w is the marker variable, the corresponding equation is f_4. The functions will be defined in Equation (3.16) in Section 3.3.4. These are the RDOA equations at each measurement time.

Walking through one example, for row one, the column one monomial is x^5. The marker variable is x, and the corresponding function is f_1. The row one label becomes

$$\frac{x^5 f_1}{x^2} = x^3 f_1 \tag{3.14}$$

Following this pattern, $\mathbf{M}$ becomes

$$\mathbf{M} = \begin{array}{c|cccccccc} & x^5 & x^4y & \ldots & xw^4 & y^5 & y^4\dot{x} & \ldots & \dot{y}w^4 & w^5 \\ \hline x^3f_1 & & & & & & & & & \\ x^2yf_1 & & & & & & & & & \\ \vdots & & & & & & & & & \\ xw^2f_4 & & & & & & & & & \\ y^3f_2 & & & & & & & & & \\ y^2\dot{x}f_2 & & & & & & & & & \\ \vdots & & & & & & & & & \\ \dot{y}w^2f_4 & & & & & & & & & \\ w^3f_4 & & & & & & & & & \end{array} \tag{3.15}$$

3.3.4 Matrix Values.

For this research, all equations have the same monomial terms but the coefficients will be different. For simplicity, f_1 will have coefficients A_i, f_2 will have B_i, f_3 C_i, and f_4 D_i.

$$\begin{aligned} f_1(x \;\; y \;\; \dot{x} \;\; w) &= A_1x^2 + A_2xy + A_3x\dot{x} + A_4xw + A_5y^2 + A_6y\dot{x} + \\ &\quad A_7yw + A_8\dot{x}^2 + A_9\dot{x}w + A_{10}w^2 \\ f_2(x \;\; y \;\; \dot{x} \;\; w) &= B_1x^2 + B_2xy + B_3x\dot{x} + B_4xw + B_5y^2 + B_6y\dot{x} + \\ &\quad B_7yw + B_8\dot{x}^2 + B_9\dot{x}w + B_{10}w^2 \\ f_3(x \;\; y \;\; \dot{x} \;\; \dot{y}) &= C_1x^2 + C_2xy + C_3x\dot{x} + C_4xw + C_5y^2 + C_6y\dot{x} + \\ &\quad C_7yw + C_8\dot{x}^2 + C_9\dot{x}w + C_{10}w^2 \\ f_4(x \;\; y \;\; \dot{x} \;\; \dot{y}) &= D_1x^2 + D_2xy + D_3x\dot{x} + D_4xw + D_5y^2 + D_6y\dot{x} + \\ &\quad D_7yw + D_8\dot{x}^2 + D_9\dot{x}w + D_{10}w^2 \end{aligned} \tag{3.16}$$

These functions are substituted for the function number in the row label. For example, in row one

$$\begin{aligned} x^3 f_1 = \; & x^3\Big[A_1x^2 + A_2xy + A_3x\dot{x} + A_4xw + A_5y^2 + A_6y\dot{x} + \\ & A_7yw + A_8\dot{x}^2 + A_9\dot{x}w + A_{10}w^2\Big] \\ = \; & A_1x^5 + A_2x^4y + A_3x^4\dot{x} + A_4x^4w + A_5x^3y^2 + A_6x^3y\dot{x} + \\ & A_7x^3yw + A_8x^3\dot{x}^2 + A_9x^3\dot{x}w + A_{10}x^3w^2 \end{aligned} \tag{3.17}$$

The coefficients from these row label equations are placed in the column matching the monomial they are multiplied by.

$$\mathbf{M} = \begin{array}{c|cccccccccc} & x^5 & x^4y & x^4\dot{x} & x^4w & x^3y^2 & x^3y\dot{x} & x^3yw & x^3\dot{x}^2 & x^3\dot{x}w & x^3w^2 \\ \hline x^3f_1 & A_1 & A_2 & A_3 & A_4 & A_5 & A_6 & A_7 & A_8 & A_9 & A_{10} \end{array}$$

See Appendix A for the full **M** matrix for the four equation, four unknown system.

3.3.5 Matrix Polynomial.

To solve for the anchor variable, the Macaulay method redefines the coefficient **M** matrix. This is seen in Equation (3.18).

$$\mathbf{M}(\dot{y}) = \mathbf{M_0} + \mathbf{M_1}\dot{y} + \mathbf{M_2}\dot{y}^2 \tag{3.18}$$

Just like Equation (3.9), $\mathbf{M_0}$, $\mathbf{M_1}$, and $\mathbf{M_2}$ are comprised of the coefficients and other variable terms from before homogenization. $\mathbf{M_0}$, $\mathbf{M_1}$, and $\mathbf{M_2}$ are the same

size as $\mathbf{M}$ but it is a way to break the coefficients down. For example,

$$\mathbf{M}(1:5,1:5) = \begin{bmatrix} A1 & A2 & A3 & A4 & A5 \\ 0 & A1 & 0 & 0 & A2 \\ 0 & 0 & A1 & 0 & 0 \\ 0 & 0 & 0 & A1 & 0 \end{bmatrix} \tag{3.19}$$

Only $A4$ has a $\dot{y}$ term. So, in terms of $\mathbf{M_0}$, $\mathbf{M_1}$, $\mathbf{M_2}$, and the coefficient breakdown in Equation (3.9), Equation (3.19) becomes

$$\mathbf{M}(1:5,1:5) = \begin{bmatrix} a1 & a2 & a3 & a5 & a6 \\ 0 & a1 & 0 & 0 & a2 \\ 0 & 0 & a1 & 0 & 0 \\ 0 & 0 & 0 & a1 & 0 \\ 0 & 0 & 0 & 0 & a1 \end{bmatrix} + \begin{bmatrix} 0 & 0 & 0 & a4 & 0 \\ 0 & 0 & 0 & 0 & 0 \\ 0 & 0 & 0 & 0 & 0 \\ 0 & 0 & 0 & 0 & 0 \\ 0 & 0 & 0 & 0 & 0 \end{bmatrix} \dot{y} + \begin{bmatrix} 0 & 0 & 0 & 0 & 0 \\ 0 & 0 & 0 & 0 & 0 \\ 0 & 0 & 0 & 0 & 0 \\ 0 & 0 & 0 & 0 & 0 \\ 0 & 0 & 0 & 0 & 0 \end{bmatrix} \dot{y}^2 \tag{3.20}$$

3.3.6 Resultant Variable Solutions.

The roots of $\mathbf{M}$ directly correspond to the eigenvalues of the companion transpose matrix.

$$\mathbf{C}^T = \begin{bmatrix} \mathbf{0} & \mathbf{I} & \mathbf{0} & \dots & \mathbf{0} \\ \mathbf{0} & \mathbf{0} & \mathbf{I} & \dots & \mathbf{0} \\ \vdots & \vdots & \dots & \vdots & \vdots \\ \mathbf{0} & \mathbf{0} & \mathbf{0} & \dots & \mathbf{I} \\ -\bar{\mathbf{M}}_{\mathbf{0}} & -\bar{\mathbf{M}}_{\mathbf{1}} & -\bar{\mathbf{M}}_{\mathbf{2}} & \dots & -\bar{\mathbf{M}}_{\mathbf{d_i-1}} \end{bmatrix} \tag{3.21}$$

Matrix inversion can be avoided by forming a generalized eigenvalue problem,

$\mathbf{A}x - \mathbf{B}$, where

$$\mathbf{A} = \begin{bmatrix} \mathbf{I} & \mathbf{0} & \mathbf{0} & \dots & \mathbf{0} \\ \mathbf{0} & \mathbf{I} & \mathbf{0} & \dots & \mathbf{0} \\ \vdots & \vdots & \dots & \vdots & \vdots \\ \mathbf{0} & \mathbf{0} & \dots & \mathbf{0} & \mathbf{0} \\ \mathbf{0} & \mathbf{0} & \dots & \mathbf{0} & \mathbf{M_{d_i}} \end{bmatrix}$$

$$\mathbf{B} = \begin{bmatrix} \mathbf{0} & \mathbf{I} & \mathbf{0} & \dots & \mathbf{0} \\ \mathbf{0} & \mathbf{0} & \mathbf{I} & \dots & \mathbf{0} \\ \vdots & \vdots & \dots & \vdots & \vdots \\ \mathbf{0} & \mathbf{0} & \mathbf{0} & \dots & \mathbf{I} \\ -\bar{\mathbf{M}}_{\mathbf{0}} & -\bar{\mathbf{M}}_{\mathbf{1}} & -\bar{\mathbf{M}}_{\mathbf{2}} & \dots & -\bar{\mathbf{M}}_{\mathbf{d_i-1}} \end{bmatrix} \tag{3.22}$$

The eigenvalues of $\mathbf{A}x - \mathbf{B}$ are the solution values of $\dot{y}$ that satisfy the original system of equations.

3.3.7 Computing Remaining Variables.

As suggested in Equation (2.11), the remaining variable solutions correspond to the kernel vector of $\mathbf{M}$ or where $\mathbf{M}(\dot{y})\mathbf{v} = \mathbf{0}$. Using a scale factor β

$$\begin{pmatrix} 1 & x & y & \dot{x} & \dot{y} & \dots & x^d & y^d & \dot{x}^d & \dot{y}^d \end{pmatrix}^T = \beta \begin{pmatrix} v_1 & v_2 & \dots & v_m \end{pmatrix} \tag{3.23}$$

Each variable solution is simply the corresponding eigenvector v_i.

3.4 Application of PSO

To use the particle swarm optimization method, a cost function must be chosen. For this astrolocalization problem, the cost function to be minimized is shown in Equation (3.24).

$$J = \|\tilde{\rho} - \rho(\mathbf{X}_T(t_0))\| \tag{3.24}$$

where $\tilde{\rho}$ is the initial transmitter state as measured by the receiver sensor. In a real-world scenario, the sensor would generate a time of arrival and RDOA would be calculated between the receivers. For the purpose of testing the solvers, an initial transmitter state will be chosen and $RDOA_{True}$ calculated from this.

Next, the solver settings must be chosen. The lower and upper bounds for the cost function are defined, as well as the particle swarm size and max number of iterations. In this use of heuristic optimization, the PSO solution will be used as an initial guess for fmincon, a MATLAB function used to find the minimum of a constrained nonlinear multivariate equation. The fmincon solution is the initial transmitter state.

3.5 Scenario Parameters

Chapter IV will walk through the localization process utilizing both Macaulay and PSO solvers for a specific example. However, the setup for any scenario will be the same:

1. Select receiver formation and transmitter orbital regime
2. Select receiver formation geometry
3. Select transmitter geometry with respect to receiver LVLH frame
4. Select measurement times
5. Propagate initial receiver and transmitter locations through chosen measurement times
6. Calculate RDOA$_{True}$ at measurement times

7. Use designated solver to determine initial transmitter state

8. The initial transmitter state is propagated to find the IROD of the transmitter

For the Macaulay solver, the coefficient matrix and matrix polynomial equation must be created. Then the eigenvalue problem can be solved to find the roots of the anchor variable. Finally, the remaining variables (and ultimately the initial transmitter state) can be computed. For the PSO solver, the cost function is defined. Then, the particle swarm parameters are set and the initial transmitter state can be computed.

3.5.1 Receiver Formations.

It is assumed that the orbits of R1 and R2 are known. Either receiver could be defined to be the chief of the LVLH frame as seen in Equation (3.25).

$$\begin{aligned} R_i &= [x,\ y,\ z,\ \dot{x},\ \dot{y},\ \dot{z}]^T \\ R_i &= [0,\ 0,\ 0,\ 0,\ 0,\ 0]^T \end{aligned} \tag{3.25}$$

Depending on the formation geometry, the initial location of either R1 or R2 can also be defined as any of the geometries in Equation (3.26) in the LVLH frame.

$$\begin{aligned} R_i &= [0,\ y,\ 0,\ 0,\ 0,\ 0]^T \ \text{ (leader/follower with y-offset)} \\ R_i &= [x,\ y,\ 0,\ 0,\ -2nx,\ 0]^T \ \text{ (NMC)} \end{aligned} \tag{3.26}$$

To account for several different types of scenarios, T can be defined as any of the

geometries in Equation (3.27) in the LVLH frame.

$$
\begin{aligned}
T &= [0,\ y,\ 0,\ 0,\ 0,\ 0]^T \ \text{(leader/follower with y-offset)} \\
T &= [x,\ y,\ 0,\ 0,\ -2nx,\ 0]^T \ \text{(NMC)} \\
T &= [x,\ y,\ 0,\ 0.001,\ 0.001,\ 0]^T \ \text{(drifting in LVLH frame)}
\end{aligned}
\tag{3.27}
$$

3.6 Summary

Chapter III has outlined the process of solving a system of polynomials to determine the location of a transmitter satellite utilizing a formation of receiver satellites. Chapter IV explores the results of specific scenarios using the algorithm developed for this research.

IV. Analysis

4.1 Result Overview

Typical geolocation (such as GPS) provides the position of an object. Typical satellite localization provides ephemeris data of the satellite in the ECI frame. This provides the orbital information to determine where the satellite will be at any given point in time. This research focuses on the IROD solution, locating a satellite with respect to another object in space utilizing the LVLH frame with HCW dynamics.

Two of the objectives of this research include analysis of receiver and transmitter geometries. The geometries chosen to be analyzed for this research are setup as shown in Figure 11. The exact geometries will be discussed in detail at the beginning of a test case scenario breakdown.

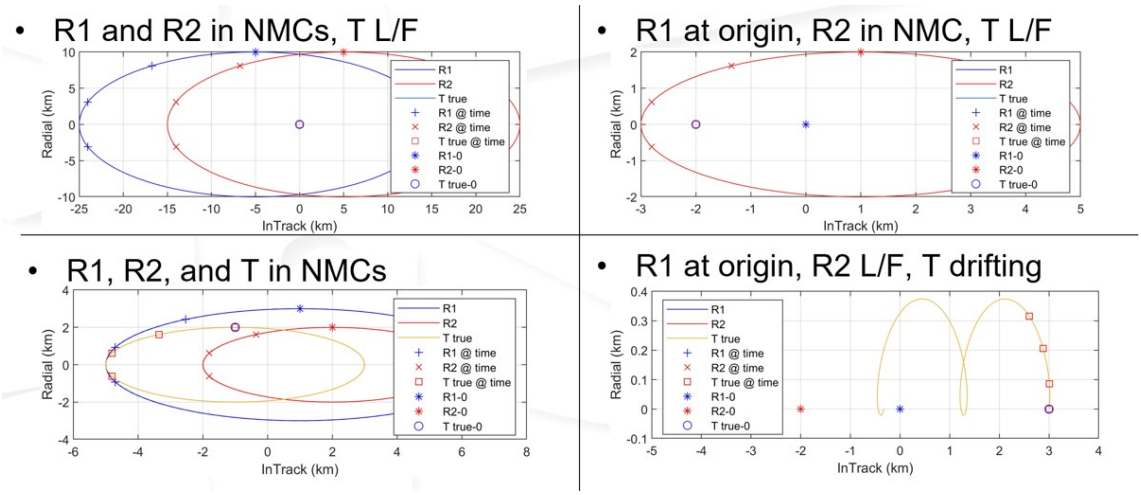

Figure 11. Example Geometries

This chapter will start by stepping through four test scenarios to show the Macaulay process and disambiguation of Macaulay solutions, as well as the PSO solutions.

4.2 Test Case 1: R1 and R2 in NMCs

For the first example, the initial LVLH reference orbit will be at an orbital altitude of 400 km. The receivers and transmitter locations in the LVLH frame are defined as $[x,\ y,\ \dot{x},\ \dot{y}]$. For example one, R1, R2, and T are defined in Equation 4.1.

$$\begin{aligned} R1 &= [10,\ -5,\ 0,\ -2nx_{R1}]^T \\ R2 &= [10,\ 5,\ 0,\ -2nx_{R2}]^T \\ T &= [0,\ 0,\ 0,\ 0]^T \end{aligned} \tag{4.1}$$

This creates a receiver geometry such that R1 is in an NMC in the LVLH frame around $(-5, 0)$ and R2 is in an NMC in the LVLH frame around $(5, 0)$. The transmitter is stationary with respect to the LVLH frame in a leader/follower formation located at $(0, 0)$ as seen in Figure 12.

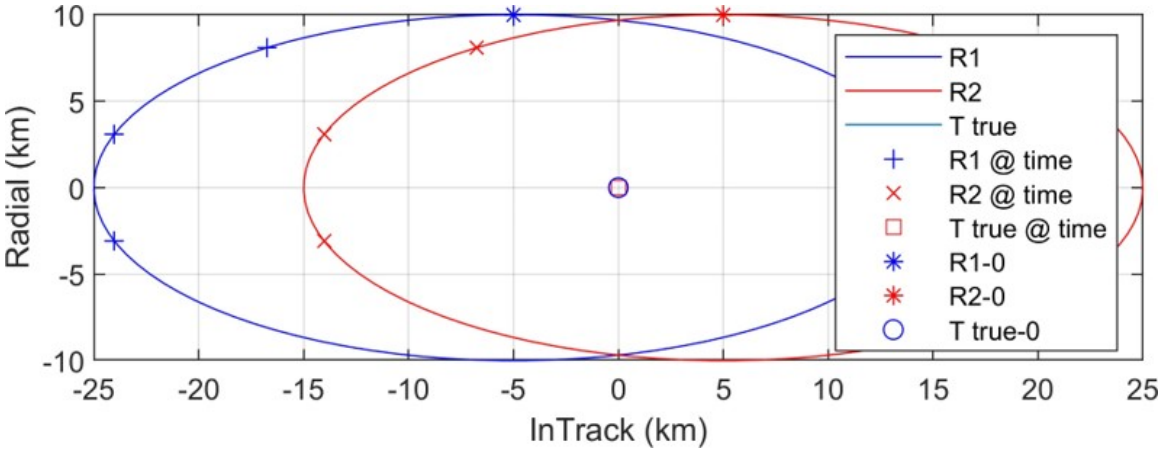

Figure 12. Example1 Setup Geometry

In a real-world scenario, the TDOA (and therefore the RDOA) is measured by a sensor on-board the receiver satellites. For this scenario, the $T_{true}(t_0)$ state is used to calculate a notional simulated RDOA measurement.

4.2.1 Test Case 1: Macaulay.

The first step in the Macaulay process (discussed in Section 3.3) is to form the coefficient matrix **M**. For the co-planar RDOA problem, there are four equations with four unknowns. Each equation is evaluated at a different time step throughout the relative orbit period. For this first example, $t = [0,\ 0.1\tau,\ 0.2\tau,\ 0.3\tau]$ where $t = 0$ is the time at which the initial transmitter and receiver orbits are defined as seen in Equation 4.1, and τ is the period of the LVLH reference orbit.

A Matlab function is written to compute the coefficients of the original system of equations based on R1, R2 and LVLH orbit parameters. The coefficient matrix for example one is shown in Table 1.

Table 1. Example1 Macaulay Coefficient Matrix

	x_t^2	$x_t y_t$	$x_t \dot{x}_t$	$x_t \dot{y}_t$	x_t	y_t^2	$y_t \dot{x}_t$	$y_t \dot{y}_t$	y_t	$\dot{x}_t^2$	$\dot{x}_t \dot{y}_t$	$\dot{x}_t$	$\dot{y}_t^2$	$\dot{y}_t$	1
t_1	0	0	0	0	0	100	0	0	0	0	0	0	0	0	0
t_2	-158.93	-16.99	0	-1.01e5	1.46e3	34.93	0	-2.36e4	821.24	0	0	0	-1.36e7	2.70e5	0
t_3	-909.07	-10.09	0	-4.90e5	1.66e3	2.7516	0	-6.72e3	104.68	0	0	0	-6.46e7	3.77e5	-7e-12
t_4	-2.23e3	-30.84	0	-7.34e5	-3.55e3	2.7516	0	-1.27e4	104.68	0	0	0	-5.40e7	-7.47e5	0

These coefficients are placed in the **M** matrix according to the process in Section 3.3.4 and the $\mathbf{M_0}$, $\mathbf{M_1}$, and $\mathbf{M_2}$ matrices are defined. Now the generalized eigenvalue problem in Equation (3.18) can be solved.

For a system of equations, the expectation is that there will be 2^n solutions, where n is the number of unknowns. Because there are four unknowns to this scenario, solving Equation (3.18) should result in 16 solutions for the anchor variable, $\dot{y}$. As described in Section 3.3.7, after the $\dot{y}$ solutions are found, the remaining variable solutions can be found by looking at the kernel of **M**. For this first example, the solutions to the Macaulay process are shown in Table 2.

Table 2. Example1 Macaulay Solutions

	True	1	2	3	4	5	6	7	8
x	0	2.498e-15	2.498e-15	2.498e-15	2.498e-15	2.498e-15	-4.2356	2.498e-15	-20.0142
y	0	2.783e-15	2.783e-15	2.783e-15	2.783e-15	2.783e-15	1.1482	2.783e-15	1.8156
$\dot{x}$	0	6.945e-15	6.945e-15	6.945e-15	6.945e-15	6.945e-15	-0.0263	6.945e-15	-0.5177
$\dot{y}$	0	0	0	0	0	0	0.0199	0	0.0891
	9	10	11	12	13	14	15	16	17
x	-3.2221	-1.6397e-14	-0.0836	-3.264e-15 -8.555e-9i	-3.264e-15 +8.555e-9i	2.498e-15	2.498e-15	2.498e-15	2.498e-15
y	0.6449	2.9141e-15	0.0295	1.968e-14 -2.139e-9i	1.968e-14 +2.139e-9i	2.783e-15	2.783e-15	2.783e-15	2.783e-15
$\dot{x}$	0.0013	1.5811e-16	-10.0874	5.0130	5.0130	6.945e-15	6.945e-15	6.945e-15	6.945e-15
$\dot{y}$	0.0157	8.1103e-17	3.1958e-4	6.920e-17 +2.822e-11i	6.920e-17 -2.822e-11i	0	0	0	0

where True is the initial value of $T(t_0)$ used to calculate the notional RDOA measurement. More analysis is needed to determine why there are 17 instead of the expected 16 solutions. Regardless of how many solutions, it is still undetermined at this point which solution is the actual location of the transmitter. A Matlab function is written to disambiguate between solutions. The disambiguation process will be shown in Section 4.2.4. Figure 13 shows the positions of the disambiguated solutions within the LVLH frame.

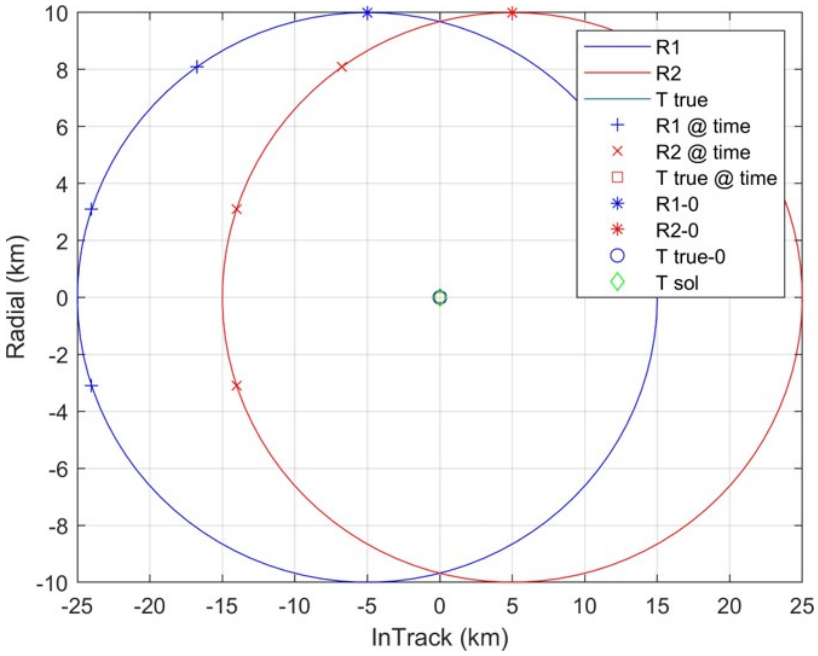

Figure 13. Example Mapped Macaulay Solutions

4.2.2 Test Case 1: PSO.

For the PSO solver, a swarm size of 500 was chosen with 100 maximum iterations. For the NMC/NMC/LF example shown Section 4.2.1 with the Macaulay process, Table 3 and Figure 14 show the PSO result.

Table 3. Example1 PSO Solution

	True	1
x	0	-9.32e-16
y	0	5.42e-16
$\dot{x}$	0	5.78e-16
$\dot{y}$	0	-4.14e-16

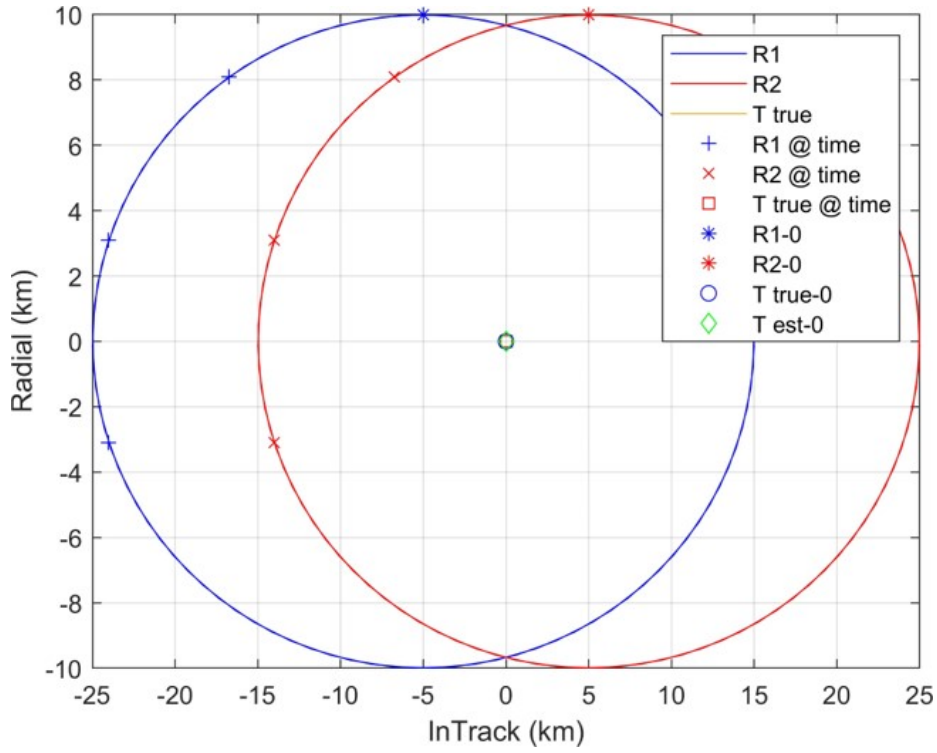

Figure 14. Example1 Mapped PSO Solution

4.2.3 Test Case 1: Discussion.

Looking at the coefficient matrix for the example (Table 1), the Macaulay matrix appears to be poorly conditioned. The coefficients range in orders of magnitude from 10^{-12} to 10^{7}. So, a scaling code that minimizes the standard deviation is applied to try to improve the method. The scaled coefficient matrix is shown in Table 4.

Table 4. Example1 Macaulay Scaled Coefficient Matrix

	x_t^2	$x_t y_t$	$x_t \dot{x}_t$	$x_t \dot{y}_t$	x_t	y_t^2	$y_t \dot{x}_t$	$y_t \dot{y}_t$	y_t	$\dot{x}_t^2$	$\dot{x}_t \dot{y}_t$	$\dot{x}_t$	$\dot{y}_t^2$	$\dot{y}_t$	1
t_1	0	0	0	0	0	5.8e10	0	0	0	0	0	0	0	0	0
t_2	-48.08	-1.39	0	-826.80	1.44e6	0.7748	0	-52.48	2.19e5	0	0	0	-3.03e3	7.23e6	0
t_3	-147.26	-0.4426	0	-2.16e3	8.74e5	0.0327	0	-8.01	1.50e4	0	0	0	-7.72e3	5.41e6	-1.3e-5
t_4	-551.58	-2.03	0	-4.84e3	-2.81e6	0.0489	0	-22.71	2.24e4	0	0	0	-9.66e3	-1.61e7	0

The solutions to the Macaulay process are shown in Table 5.

Table 5. Example1 Macaulay Scaled Solutions

	True	1	2	3	4	5	6	7	8	9	10
x	0	6.1807e-9	6.1807e-9	6.1807e-9	6.1807e-9	6.1807e-9	-2.3607	6.1807e-9	-1.5211e4	-0.0057	4.0229e3
y	0	-5.3407e-8	-5.3407e-8	-5.3407e-8	-5.3407e-8	-5.3407e-8	-0.1851	-53407e-8	0.0612	-0.0813	-1.2948
$\dot{x}$	0	1.3291e-5	1.3291e-5	1.3291e-5	1.3291e-5	1.3291e-5	-0.2860	1.3291e-5	12.4131	-0.2505	97.5238
$\dot{y}$	0	0	0	0	0	0	2.3836e3	0	2.7509e3	3.1828e-4	1.6606e3
	11	12	13	14	15	16	17	18	19	20	
x	-6.2844e4	-7.4018e3	8.1482e-10	-9.7301e-10	-7.6430e-7	1.5855e-6	6.1807e-9	6.1807e-9	6.1807e-9	6.1807e-9	
y	83.6469	-1.8497e4	-4.8217e-9	-2.0015e-10	-2.0919e-6	-1.3943e-6	-5.3407e-8	-5.3407e-8	-5.3407e-8	-5.3407e-8	
$\dot{x}$	-3.0127e7	-2.4397e-17	4.0333e-8	-2.3811e-9	-0.0089	-0.0390	1.3291e-5	1.3291e-5	1.3291e-5	1.3291e-5	
$\dot{y}$	1.0699e4	1.8856e3	-4.8740e-11	1.8924e-10	1.9223e-7	-1.9220e-7	0	0	0	0	

It is unclear, however, if this improves the accuracy of the results. A clear set of metrics to analyze results is needed to disambiguate the solutions.

4.2.4 Test Case 1: Disambiguation of Macaulay Solutions.

Starting with the solutions that solve the generalized eigenvalue problem, the first filter applied pulls out the solutions that have "big" imaginary parts. The location of the transmitter is a real location. It is possible that a small imaginary part in the solutions is due to machine precision, however, a solution with a bigger imaginary part is less likely to be the location of the transmitter. The second filter pulls out the duplicate solutions. Analysis only needs to be done on one of these solutions. The third filter examines the polynomials constructed from the coefficient matrices. Each row of the coefficient matrix is an RDOA equation at a specific measurement time. Solutions that have passed the first two filters are propagated over time to find their relative locations at the measurement times and are then plugged into the polynomials. These values are compared to the polynomial solutions utilizing the True transmitter initial values. The fourth filter plugs the remaining solutions into the initial RDOA equation (Equation (3.1)). These are compared to the True transmitter initial values. The fifth filter looks at the solutions in their inertial orbits.

Due to the use of HCW dynamics, the solution orbits cannot be far outside the initial LVLH orbit. It is expected that the solution orbits will be within the same orbital regime as the initial LVLH orbit. The last filter examines the perigee of the solution orbits. The perigee needs to be outside the radius of the Earth for the orbit not to be ballistic.

These six filters are applied to the example and the remaining solutions analyzed. For the unscaled Macaulay scenario, there are two solutions remaining. For the scaled Macaulay scenario, there are five solutions remaining after disambiguation. The PSO scenario solved for one optimal solution. The results of the disambiguation filters are shown in Table 6.

Table 6. Example1 LEO Macaulay Disambiguation

	Solutions Left After Check - Unscaled	Solutions Left After Check - Scaled
Total Solutions out of Macaulay Solver	112	112
Step 1: Infinity Check	17	20
Step 2: Imaginary Check	17	20
Step 3: Duplicate Check	8	11
Step 4: Polynomial Check	4	5
Step 5: RDOA Check	4	5
Step 6: Orbit Check1 - logical orbital regime	3	5
Step 7: Orbit Check2 - perigee check	2	5

The IROD accuracy is shown in Table 7.

$$\text{IROD Accuracy} \;=\; \|\mathbf{X}_{True}(t_0) - \mathbf{X}_{Sol}(t_0)\|$$

Table 7. Example1 LEO IROD Summary

Solution	Position Error (km)	Velocity Error (km/s)
1	3.7395e-15	6.9447e-15
10	1.6654e-14	1.7770e-16
Unscaled 17 solutions, 2 remaining		
Solution	Position Error (km)	Velocity Error (km/s)
1	5.3764e-8	1.3291e-5
11	6.7935e-8	0.1056
12	6.8590e-8	0.0036
13	1.6597e-6	4.3445e-4
14	4.8613e-6	0.0016
Scaled 20 solutions, 5 remaining		
Solution	Position Error (km)	Velocity Error (km/s)
1	1.3729e-16	8.4834e-16
PSO		

Examining the same LVLH geometry at GEO instead of LEO where the orbital altitude is 35786 km, this scenario is disambiguated as shown in Table 8 and the IROD results are seen in Table 9.

Table 8. Example1 GEO Macaulay Disambiguation

	Solutions Left After Check - Unscaled	Solutions Left After Check - Scaled
Total Solutions out of Macaulay Solver	112	112
Step 1: Infinity Check	25	24
Step 2: Imaginary Check	25	24
Step 3: Duplicate Check	12	11
Step 4: Polynomial Check	4	2
Step 5: RDOA Check	4	0
Step 6: Orbit Check1 - logical orbital regime	2	
Step 7: Orbit Check2 - perigee check	2	

Table 9. Example1 GEO IROD Summary

Solution	Position Error (km)	Velocity Error (km/s)
1	5.1451e-15	1.0671e-14
10	1.1415e-14	9.1301e-15
Unscaled 25 solutions, 2 remaining		
Solution	Position Error (km)	Velocity Error (km/s)
0	No solution found	
Scaled 24 solutions, 0 remaining		
Solution	Position Error (km)	Velocity Error (km/s)
1	6.4042e-16	9.7077e-16
PSO		

As seen in Table 9, the scaled Macaulay code filters out all possible solutions and no realistic IROD is found.

4.3 Test Case 2: R1 at origin and R2 in NMC

For the second example, the initial LVLH reference orbit will be set as follows

$$\text{alt} = 400 \text{ km} \tag{4.2}$$

And the receivers and transmitter locations in the LVLH frame will be

$$\begin{aligned} R1 &= [0,\ 0,\ 0,\ 0]^T \\ R2 &= [2,\ 1,\ 0,\ -2nx_{R2}]^T \\ T &= [0,\ -2,\ 0,\ 0]^T \end{aligned} \tag{4.3}$$

This creates a receiver geometry such that R1 is stationary in the LVLH frame in a leader/follower formation located at $(0, 0)$ and R2 is in an NMC in the LVLH frame around $(1, 0)$. The transmitter is stationary with respect to the LVLH frame in a leader/follower formation located at $(-2, 0)$ as seen in Figure 15.

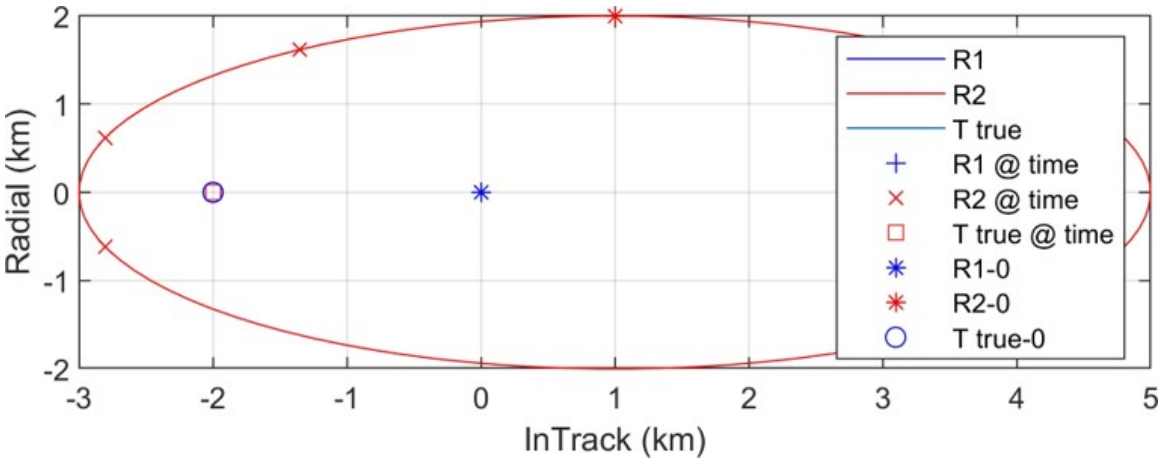

Figure 15. Example2 Setup Geometry

The Macaulay disambiguation results are shown in Table 10 and the IROD results for this LEO scenario are seen in Table 11.

Table 10. Example2 LEO Macaulay Disambiguation

	Solutions Left After Check - Unscaled	Solutions Left After Check - Scaled
Total Solutions out of Macaulay Solver	112	112
Step 1: Infinity Check	16	16
Step 2: Imaginary Check	16	16
Step 3: Duplicate Check	13	13
Step 4: Polynomial Check	8	3
Step 5: RDOA Check	7	3
Step 6: Orbit Check1 - logical orbital regime	4	3
Step 7: Orbit Check2 - perigee check	4	3

Table 11. Example2 LEO IROD Summary

Solution	Position Error (km)	Velocity Error (km/s)
6	2.2990	0.1457
11	3.9364	0.0380
15	0.7862	0.0843
16	0.7862	0.0843
Unscaled 16 solutions, 4 remaining		
Solution	Position Error (km)	Velocity Error (km/s)
1	0.4533	0.3316
9	0.4533	0.0851
14	0.4533	0.1232
Scaled 16 solutions, 3 remaining		
Solution	Position Error (km)	Velocity Error (km/s)
1	8.8818e-16	7.6246e-16
PSO		

If the scenario is located in GEO instead of LEO, the altitude becomes 35786 km.

The Macaulay disambiguation is shown in Table 12 and the IROD results for this GEO scenario are seen in Table 13.

Table 12. Example2 GEO Macaulay Disambiguation

	Solutions Left After Check - Unscaled	Solutions Left After Check - Scaled
Total Solutions out of Macaulay Solver	112	112
Step 1: Infinity Check	16	18
Step 2: Imaginary Check	16	14
Step 3: Duplicate Check	13	11
Step 4: Polynomial Check	6	3
Step 5: RDOA Check	6	3
Step 6: Orbit Check1 - logical orbital regime	2	0
Step 7: Orbit Check2 - perigee check	2	

Table 13. Example2 GEO IROD Summary

Solution	Position Error (km)	Velocity Error (km/s)
15	0.8794	0.1627
16	0.8794	0.1627
Unscaled 16 solutions, 2 remaining		
Solution	Position Error (km)	Velocity Error (km/s)
0	No solution found	
Scaled 18 solutions, 0 remaining		
Solution	Position Error (km)	Velocity Error (km/s)
1	8.8818e-16	7.8319e-16
PSO		

Again, as seen in Table 13, the scaled Macaulay code filters out all possible solutions for the GEO scenario and no realistic IROD is found.

4.4 Test Case 3: R1 and R2 in NMCs

For the third example, the initial LVLH orbit will be set as follows

$$\text{alt} = 400 \text{ km} \tag{4.4}$$

And the receivers and transmitter locations in the LVLH frame will be

$$\begin{aligned} R1 &= [3,\ 1,\ 0,\ -2nx_{R1}]^T \\ R2 &= [2,\ 2,\ 0,\ -2nx_{R2}]^T \\ T &= [2,\ -1,\ 0,\ -2nx_T]^T \end{aligned} \tag{4.5}$$

This creates a receiver geometry such that R1 is in an NMC in the LVLH frame around $(1, 0)$ and R2 is in an NMC in the LVLH frame around $(2, 0)$. The transmitter is also in an NMC in the LVLH frame around $(-1, 0)$ as seen in Figure 16.

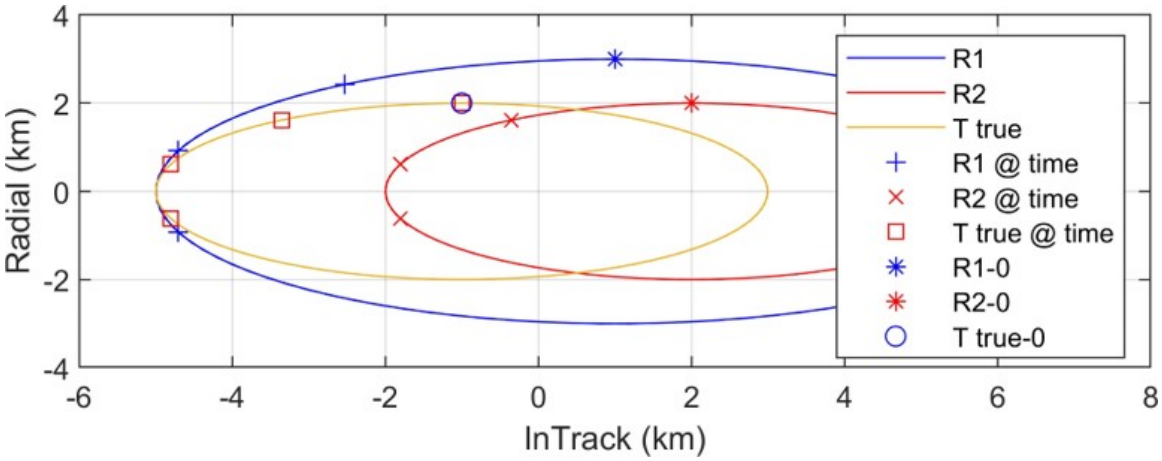

Figure 16. Example3 Setup Geometry

The Macaulay disambiguation results are shown in Table 14 and the IROD results for this LEO scenario are shown in Table 15.

Table 14. Example3 LEO Macaulay Disambiguation

	Solutions Left After Check - Unscaled	Solutions Left After Check - Scaled
Total Solutions out of Macaulay Solver	112	112
Step 1: Infinity Check	17	16
Step 2: Imaginary Check	17	14
Step 3: Duplicate Check	14	11
Step 4: Polynomial Check	1	0
Step 5: RDOA Check	1	
Step 6: Orbit Check1 - logical orbital regime	1	
Step 7: Orbit Check2 - perigee check	1	

Table 15. Example3 LEO IROD Summary

Solution	Position Error (km)	Velocity Error (km/s)
13	3.0902	0.0759
Unscaled 17 solutions, 1 remaining		
Solution	Position Error (km)	Velocity Error (km/s)
0	No solution found	
Scaled 16 solutions, 0 remaining		
Solution	Position Error (km)	Velocity Error (km/s)
1	9.4206e-16	0.0045
PSO		

If the scenario is located in GEO instead of LEO, the altitude becomes 35786 km. The Macaulay disambiguation is shown in Table 16 and the IROD results are seen in Table 17.

Table 16. Example3 GEO Macaulay Disambiguation

	Solutions Left After Check - Unscaled	Solutions Left After Check - Scaled
Total Solutions out of Macaulay Solver	112	112
Step 1: Infinity Check	16	16
Step 2: Imaginary Check	16	14
Step 3: Duplicate Check	13	11
Step 4: Polynomial Check	0	0
Step 5: RDOA Check		
Step 6: Orbit Check1 - logical orbital regime		
Step 7: Orbit Check2 - perigee check		

Table 17. Example3 GEO IROD Summary

Solution	Position Error (km)	Velocity Error (km/s)
0	No solution found	
Unscaled 16 solutions, 0 remaining		
Solution	Position Error (km)	Velocity Error (km/s)
0	No solution found	
Scaled 16 solutions, 0 remaining		
Solution	Position Error (km)	Velocity Error (km/s)
1	4.4409e-16	2.9169e-4
PSO		

The scaled Macaulay code filters out all possible solutions for the LEO and GEO scenario and no realistic IROD is found. Even the unscaled Macaulay code filters out all possible solutions for the GEO scenario and no realistic IROD is found.

4.5 Test Case 4: R1 and R2 at stationary LVLH point

For the fourth example, the initial LVLH orbit will be set as follows

$$\text{alt} = 400 \text{ km} \tag{4.6}$$

And the receivers and transmitter locations in the LVLH frame will be

$$\begin{aligned} R1 &= [0,\ 0,\ 0,\ 0]^T \\ R2 &= [0,\ -2,\ 0,\ 0]^T \\ T &= [0,\ 3,\ 0.0001,\ 0.0001]^T \end{aligned} \tag{4.7}$$

This creates a receiver geometry such that R1 is stationary with respect to the LVLH frame in a leader/follower formation located at $(0, 0)$ and R2 is stationary with respect to the LVLH frame in a leader/follower formation located at $(-2, 0)$. The transmitter is drifting with respect to the LVLH frame starting at $(3, 0)$ as seen in Figure 17.

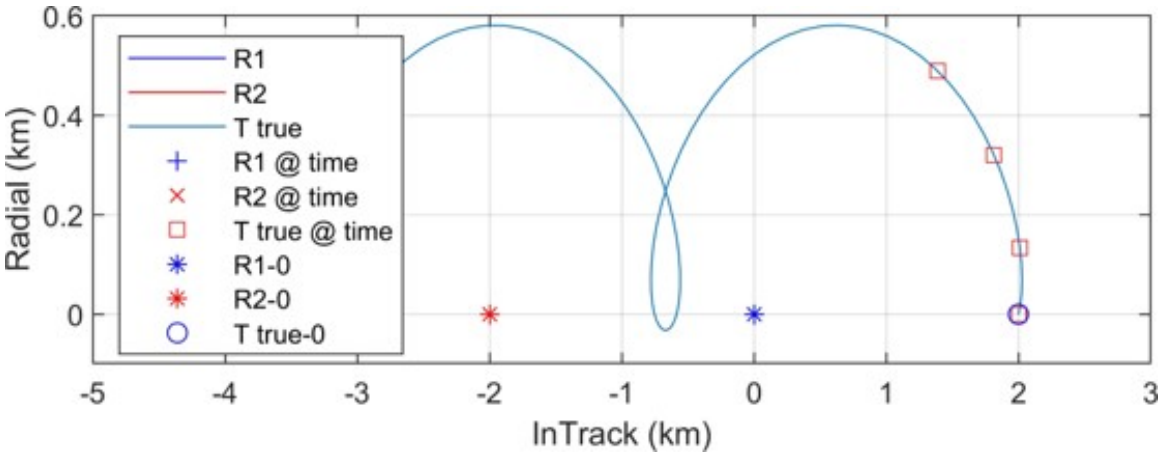

Figure 17. Example4 Setup Geometry

The Macaulay disambiguation results are shown in Table 18 and the IROD results for this LEO scenario are shown in Table 19.

Table 18. Example4 LEO Macaulay Disambiguation

	Solutions Left After Check - Unscaled	Solutions Left After Check - Scaled
Total Solutions out of Macaulay Solver	112	112
Step 1: Infinity Check	21	23
Step 2: Imaginary Check	15	19
Step 3: Duplicate Check	15	19
Step 4: Polynomial Check	13	0
Step 5: RDOA Check	8	
Step 6: Orbit Check1 - logical orbital regime	5	
Step 7: Orbit Check2 - perigee check	2	

Table 19. Example4 LEO IROD Summary

Solution	Position Error (km)	Velocity Error (km/s)
9	3.3800	0.0231
20	3.0038	0.0930
Unscaled 21 solutions, 2 remaining		
Solution	Position Error (km)	Velocity Error (km/s)
0	No solution found	
Scaled 23 solutions, 0 remaining		
Solution	Position Error (km)	Velocity Error (km/s)
1	4.4409e-16	1.4142e-4
PSO		

If the scenario is located in GEO instead of LEO, the altitude becomes 35786 km. The Macaulay disambiguation is shown in Table 20 and the IROD results are shown in Table 21.

Table 20. Example4 GEO Macaulay Disambiguation

	Solutions Left After Check - Unscaled	Solutions Left After Check - Scaled
Total Solutions out of Macaulay Solver	112	112
Step 1: Infinity Check	28	24
Step 2: Imaginary Check	22	16
Step 3: Duplicate Check	22	16
Step 4: Polynomial Check	8	0
Step 5: RDOA Check	7	
Step 6: Orbit Check1 - logical orbital regime	0	
Step 7: Orbit Check2 - perigee check		

Table 21. Example4 GEO IROD Summary

Solution	Position Error (km)	Velocity Error (km/s)
0	No solution found	
Unscaled 28 solutions, 0 remaining		
Solution	Position Error (km)	Velocity Error (km/s)
0	No solution found	
Scaled 24 solutions, 0 remaining		
Solution	Position Error (km)	Velocity Error (km/s)
1	4.7054e-16	1.4142e-4
PSO		

Again, the scaled Macaulay code filters out all possible solutions for the LEO and GEO scenario and no realistic IROD is found. Even the unscaled Macaulay code filters out all possible solutions for the GEO scenario and no realistic IROD is found.

4.6 Formation Analysis

Two of the objectives of this research include analysis of receiver and transmitter geometries. The geometries chosen to be analyzed for this research are setup as shown in Figure 18.

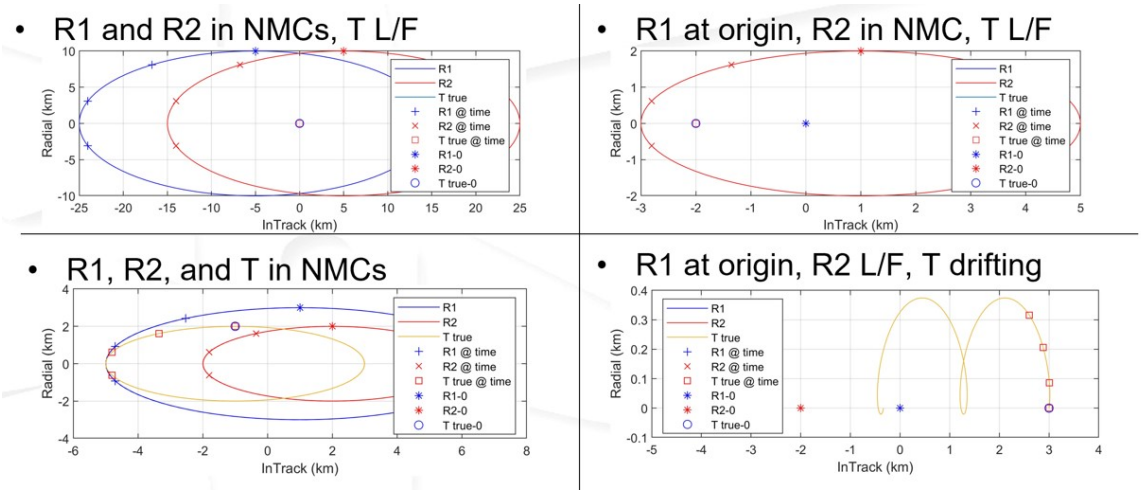

Figure 18. Example Geometries

Examining the geometries, placing both receivers in NMCs seems to accomplish astrolocation to a certain degree. Scenario one is solved with very little error. However, the Macualay solver cannot solve scenario three at GEO. Placing one receiver in an NMC and another stationary in the LVLH frame shows some promising results as scenario two is solved. However, placing both receivers stationary in the LVLH frame seems to yield no results.

From the limited scenarios examined, it appears that the Macaulay solver performs better with a stationary transmitter (or setting the LVLH frame at the transmitter). For scenario one and scenario two, the transmitter was astrolocated despite different orbital regimes and different receiver formations.

As far as orbital regime, it appears that GEO makes solving the IROD problem with Macaulay difficult. The PSO solver doesn't seem to have the same problem.

4.7 Summary

Chapter IV explored the results of specific scenarios using the algorithm developed for this research. Chapter V concludes the research with summarized results and contributions along with recommendations for future research.

V. Conclusions

5.1 Research Summary

The research accomplished here is ground breaking in terms of the use of the Macaulay resultant method for IROD. A MATLAB simulation was developed to analyze the polynomial solvers, different receiver formation geometries and how well those receiver geometries solve the astrolocation problem, as well as analyze the geometry between the receivers and the transmitter including orbital regime.

This research sought to draw conclusions about astrolocation in general by asking the following questions:

- Given two cooperative receivers, what formation geometries are effective or ineffective at astrolocating a transmitter?
- Given a formation geometry for two cooperative receivers, what are potential transmitter geometries for which IROD is possible?
- And given a geometry between receivers and a transmitter, how does the orbital regime influence the IROD solution?

In general, this research has shown that both the Macaulay resultant method and the PSO method can solve for IROD of an orbiting transmitter using two receivers in a formation. Chapter V will examine the conclusions drawn about specific geometries examined in Chapter IV.

5.2 Receiver Formation Geometries

This research sought to answer the following question: given two cooperative receivers, what formation geometries are effective or ineffective at astrolocating a

transmitter? Based on the example scenarios presented in Chapter IV, it appears that an IROD solution is more likely to be found by the Macaulay method when one receiver is stationary and one is moving in the LVLH frame. However, there were scenarios where the IROD problem could not be solved, and the cause of the lack of solution cannot be ascertained. The PSO method had no trouble computing the IROD regardless of receiver formation.

5.3 Transmitter Relative Geometries

This research sought to answer the following question: given a formation geometry for two cooperative receivers, what are potential transmitter geometries for which IROD is possible? Based on the example scenarios presented in Chapter IV, it appears that an IROD solution is more likely to be found by the Macaulay method when the transmitter is stationary with respect to the LVLH frame. The PSO method had no trouble computing the IROD regardless of transmitter formation geometry.

5.4 Orbital Regimes

This research sought to answer the following question: given a geometry between receivers and a transmitter, how does the orbital regime influence the IROD solution? Based on the example scenarios presented in Chapter IV, it appears that an IROD solution is less likely to be found by the Macaulay method when the receivers and transmitter are located at GEO. The PSO method had no trouble computing the IROD regardless of orbital regime.

5.5 Future Work

This research found that the Macaulay method can be used for IROD, but there seem to be some limitations with the parameters that were chosen.

- HCW dynamics were used. Utilizing different STM dynamics that allow for more eccentric chief orbits or include perturbation effects could provide a more realistic estimated trajectory.

- This research used one set of measurement times that were specific fractions of the LVLH orbit period. Measurement times could be optimized to provide better geometry relationships between R1 and R2. [17] found that the greater the angle between receivers, the more accurate the location solution.

- This research did not include cross-track motion in the Macaulay solver method. The cross-track motion adds a whole new set of challenges. The Macaulay method would need to be restarted and $\mathbf{M}$ redefined based on the new RDOA equations.

- This research only utilized a TDOA signal processing technique. By taking a hybrid approach to processing and adding an AOA or FDOA technique to the TDOA measurements, more data can be gathered about a specific location and more accurate estimates could be made. However, the Macaulay method would need to be restarted and $\mathbf{M}$ redefined based on the new measurement equations.

- This research began with a coarse disambiguation process for the Macaulay solver. The disambiguation process should be expanded and refined.

- This research did not address the observability of the transmitter states. It is possible that the observability of the transmitter would provide further insight into the results presented in Chapter IV.

5.6 Analysis

The goal of this research was to examine the feasibility of the Macaulay method for IROD as well as enhance SDA methods. TDOA IROD would be an excellent secondary mission for a formation of satellites. While the formation is performing a primary mission, the formation satellites could also have receivers collecting opportunistic data as other satellites downlink to ground stations. This data could be used to augment current SDA methods.

Appendix A. Macaulay M matrix

The Macaulay coefficient matrix defined in Section 3.3 is

$$
M = \begin{matrix}
A1 & A2 & A3 & A4 & A5 & A6 & A7 & A8 & A9 & A10 & 0 & 0 & 0 & 0 & 0 & 0 & 0 & 0 & 0 & 0 & 0 & 0 & 0 & 0 & 0 & 0 & 0 & 0 & 0 & 0 & 0 & 0 & 0 & 0 & 0 & 0 & 0 & 0 & 0 & 0 & 0 & 0 & 0 & 0 & 0 & 0 & 0 & 0 & 0 & 0 & 0 & 0 & 0 & 0 & 0 & 0 \\
0 & A1 & 0 & 0 & A2 & A3 & A4 & 0 & 0 & 0 & A5 & A6 & A7 & A8 & A9 & A10 & 0 & 0 & 0 & 0 & 0 & 0 & 0 & 0 & 0 & 0 & 0 & 0 & 0 & 0 & 0 & 0 & 0 & 0 & 0 & 0 & 0 & 0 & 0 & 0 & 0 & 0 & 0 & 0 & 0 & 0 & 0 & 0 & 0 & 0 & 0 & 0 & 0 & 0 & 0 & 0 \\
0 & 0 & A1 & 0 & 0 & A2 & 0 & A3 & A4 & 0 & 0 & A5 & 0 & A6 & A7 & 0 & A8 & A9 & A10 & 0 & 0 & 0 & 0 & 0 & 0 & 0 & 0 & 0 & 0 & 0 & 0 & 0 & 0 & 0 & 0 & 0 & 0 & 0 & 0 & 0 & 0 & 0 & 0 & 0 & 0 & 0 & 0 & 0 & 0 & 0 & 0 & 0 & 0 & 0 & 0 & 0 \\
0 & 0 & 0 & A1 & 0 & 0 & A2 & 0 & A3 & A4 & 0 & 0 & A5 & 0 & A6 & A7 & 0 & A8 & A9 & A10 & 0 & 0 & 0 & 0 & 0 & 0 & 0 & 0 & 0 & 0 & 0 & 0 & 0 & 0 & 0 & 0 & 0 & 0 & 0 & 0 & 0 & 0 & 0 & 0 & 0 & 0 & 0 & 0 & 0 & 0 & 0 & 0 & 0 & 0 & 0 & 0 \\
0 & 0 & 0 & 0 & A1 & 0 & 0 & 0 & 0 & 0 & A2 & A3 & A4 & 0 & 0 & 0 & 0 & 0 & 0 & 0 & A5 & A6 & A7 & A8 & A9 & A10 & 0 & 0 & 0 & 0 & 0 & 0 & 0 & 0 & 0 & 0 & 0 & 0 & 0 & 0 & 0 & 0 & 0 & 0 & 0 & 0 & 0 & 0 & 0 & 0 & 0 & 0 & 0 & 0 & 0 & 0 \\
0 & 0 & 0 & 0 & 0 & A1 & 0 & 0 & 0 & 0 & 0 & A2 & 0 & A3 & A4 & 0 & 0 & 0 & 0 & 0 & 0 & A5 & 0 & A6 & A7 & 0 & A8 & A9 & A10 & 0 & 0 & 0 & 0 & 0 & 0 & 0 & 0 & 0 & 0 & 0 & 0 & 0 & 0 & 0 & 0 & 0 & 0 & 0 & 0 & 0 & 0 & 0 & 0 & 0 & 0 & 0 \\
0 & 0 & 0 & 0 & 0 & 0 & A1 & 0 & 0 & 0 & 0 & 0 & A2 & 0 & A3 & A4 & 0 & 0 & 0 & 0 & 0 & 0 & A5 & 0 & A6 & A7 & 0 & A8 & A9 & A10 & 0 & 0 & 0 & 0 & 0 & 0 & 0 & 0 & 0 & 0 & 0 & 0 & 0 & 0 & 0 & 0 & 0 & 0 & 0 & 0 & 0 & 0 & 0 & 0 & 0 & 0 \\
0 & 0 & 0 & 0 & 0 & 0 & 0 & A1 & 0 & 0 & 0 & 0 & 0 & A2 & 0 & 0 & A3 & A4 & 0 & 0 & 0 & 0 & 0 & A5 & 0 & 0 & A6 & A7 & 0 & 0 & A8 & A9 & A10 & 0 & 0 & 0 & 0 & 0 & 0 & 0 & 0 & 0 & 0 & 0 & 0 & 0 & 0 & 0 & 0 & 0 & 0 & 0 & 0 & 0 & 0 & 0 \\
0 & 0 & 0 & 0 & 0 & 0 & 0 & 0 & A1 & 0 & 0 & 0 & 0 & 0 & A2 & 0 & 0 & A3 & A4 & 0 & 0 & 0 & 0 & 0 & A5 & 0 & 0 & A6 & A7 & 0 & 0 & A8 & A9 & A10 & 0 & 0 & 0 & 0 & 0 & 0 & 0 & 0 & 0 & 0 & 0 & 0 & 0 & 0 & 0 & 0 & 0 & 0 & 0 & 0 & 0 & 0 \\
0 & 0 & 0 & 0 & 0 & 0 & 0 & 0 & 0 & A1 & 0 & 0 & 0 & 0 & 0 & A2 & 0 & 0 & A3 & A4 & 0 & 0 & 0 & 0 & 0 & A5 & 0 & 0 & A6 & A7 & 0 & 0 & A8 & A9 & A10 & 0 & 0 & 0 & 0 & 0 & 0 & 0 & 0 & 0 & 0 & 0 & 0 & 0 & 0 & 0 & 0 & 0 & 0 & 0 & 0 & 0 \\
0 & 0 & 0 & 0 & 0 & 0 & 0 & 0 & 0 & 0 & A1 & 0 & 0 & 0 & 0 & 0 & 0 & 0 & 0 & 0 & A2 & A3 & A4 & 0 & 0 & 0 & 0 & 0 & 0 & 0 & 0 & 0 & 0 & 0 & 0 & A5 & A6 & A7 & A8 & A9 & A10 & 0 & 0 & 0 & 0 & 0 & 0 & 0 & 0 & 0 & 0 & 0 & 0 & 0 & 0 & 0 \\
0 & 0 & 0 & 0 & 0 & 0 & 0 & 0 & 0 & 0 & 0 & A1 & 0 & 0 & 0 & 0 & 0 & 0 & 0 & 0 & 0 & A2 & 0 & A3 & A4 & 0 & 0 & 0 & 0 & 0 & 0 & 0 & 0 & 0 & 0 & 0 & A5 & 0 & A6 & A7 & 0 & A8 & A9 & A10 & 0 & 0 & 0 & 0 & 0 & 0 & 0 & 0 & 0 & 0 & 0 & 0 \\
0 & 0 & 0 & 0 & 0 & 0 & 0 & 0 & 0 & 0 & 0 & 0 & A1 & 0 & 0 & 0 & 0 & 0 & 0 & 0 & 0 & 0 & A2 & 0 & A3 & A4 & 0 & 0 & 0 & 0 & 0 & 0 & 0 & 0 & 0 & 0 & 0 & A5 & 0 & A6 & A7 & 0 & A8 & A9 & A10 & 0 & 0 & 0 & 0 & 0 & 0 & 0 & 0 & 0 & 0 & 0 \\
0 & 0 & 0 & 0 & 0 & 0 & 0 & 0 & 0 & 0 & 0 & 0 & 0 & A1 & 0 & 0 & 0 & 0 & 0 & 0 & 0 & 0 & 0 & A2 & 0 & 0 & A3 & A4 & 0 & 0 & 0 & 0 & 0 & 0 & 0 & 0 & 0 & 0 & A5 & 0 & 0 & A6 & A7 & 0 & 0 & A8 & A9 & A10 & 0 & 0 & 0 & 0 & 0 & 0 & 0 & 0 \\
0 & 0 & 0 & 0 & 0 & 0 & 0 & 0 & 0 & 0 & 0 & 0 & 0 & 0 & A1 & 0 & 0 & 0 & 0 & 0 & 0 & 0 & 0 & 0 & A2 & 0 & 0 & A3 & A4 & 0 & 0 & 0 & 0 & 0 & 0 & 0 & 0 & 0 & 0 & A5 & 0 & 0 & A6 & A7 & 0 & 0 & A8 & A9 & A10 & 0 & 0 & 0 & 0 & 0 & 0 & 0 \\
0 & 0 & 0 & 0 & 0 & 0 & 0 & 0 & 0 & 0 & 0 & 0 & 0 & 0 & 0 & A1 & 0 & 0 & 0 & 0 & 0 & 0 & 0 & 0 & 0 & A2 & 0 & 0 & A3 & A4 & 0 & 0 & 0 & 0 & 0 & 0 & 0 & 0 & 0 & 0 & A5 & 0 & 0 & A6 & A7 & 0 & 0 & A8 & A9 & A10 & 0 & 0 & 0 & 0 & 0 & 0 \\
0 & 0 & 0 & 0 & 0 & 0 & 0 & 0 & 0 & 0 & 0 & 0 & 0 & 0 & 0 & 0 & A1 & 0 & 0 & 0 & 0 & 0 & 0 & 0 & 0 & 0 & A2 & 0 & 0 & 0 & A3 & A4 & 0 & 0 & 0 & 0 & 0 & 0 & 0 & 0 & 0 & A5 & 0 & 0 & 0 & A6 & A7 & 0 & 0 & 0 & A8 & A9 & A10 & 0 & 0 & 0 \\
0 & 0 & 0 & 0 & 0 & 0 & 0 & 0 & 0 & 0 & 0 & 0 & 0 & 0 & 0 & 0 & 0 & A1 & 0 & 0 & 0 & 0 & 0 & 0 & 0 & 0 & 0 & A2 & 0 & 0 & 0 & A3 & A4 & 0 & 0 & 0 & 0 & 0 & 0 & 0 & 0 & 0 & A5 & 0 & 0 & 0 & A6 & A7 & 0 & 0 & 0 & A8 & A9 & A10 & 0 & 0 \\
0 & 0 & 0 & 0 & 0 & 0 & 0 & 0 & 0 & 0 & 0 & 0 & 0 & 0 & 0 & 0 & 0 & 0 & A1 & 0 & 0 & 0 & 0 & 0 & 0 & 0 & 0 & 0 & A2 & 0 & 0 & 0 & A3 & A4 & 0 & 0 & 0 & 0 & 0 & 0 & 0 & 0 & 0 & A5 & 0 & 0 & 0 & A6 & A7 & 0 & 0 & 0 & A8 & A9 & A10 & 0 \\
0 & 0 & 0 & 0 & 0 & 0 & 0 & 0 & 0 & 0 & 0 & 0 & 0 & 0 & 0 & 0 & 0 & 0 & 0 & A1 & 0 & 0 & 0 & 0 & 0 & 0 & 0 & 0 & 0 & A2 & 0 & 0 & 0 & A3 & A4 & 0 & 0 & 0 & 0 & 0 & 0 & 0 & 0 & 0 & A5 & 0 & 0 & 0 & A6 & A7 & 0 & 0 & 0 & A8 & A9 & A10 \\
0 & 0 & 0 & 0 & B1 & 0 & 0 & 0 & 0 & 0 & B2 & B3 & B4 & 0 & 0 & 0 & 0 & 0 & 0 & 0 & B5 & B6 & B7 & B8 & B9 & B10 & 0 & 0 & 0 & 0 & 0 & 0 & 0 & 0 & 0 & 0 & 0 & 0 & 0 & 0 & 0 & 0 & 0 & 0 & 0 & 0 & 0 & 0 & 0 & 0 & 0 & 0 & 0 & 0 & 0 & 0 \\
0 & 0 & 0 & 0 & 0 & B1 & 0 & 0 & 0 & 0 & 0 & B2 & 0 & B3 & B4 & 0 & 0 & 0 & 0 & 0 & 0 & B5 & 0 & B6 & B7 & 0 & B8 & B9 & B10 & 0 & 0 & 0 & 0 & 0 & 0 & 0 & 0 & 0 & 0 & 0 & 0 & 0 & 0 & 0 & 0 & 0 & 0 & 0 & 0 & 0 & 0 & 0 & 0 & 0 & 0 & 0 \\
0 & 0 & 0 & 0 & 0 & 0 & B1 & 0 & 0 & 0 & 0 & 0 & B2 & 0 & B3 & B4 & 0 & 0 & 0 & 0 & 0 & 0 & B5 & 0 & B6 & B7 & 0 & B8 & B9 & B10 & 0 & 0 & 0 & 0 & 0 & 0 & 0 & 0 & 0 & 0 & 0 & 0 & 0 & 0 & 0 & 0 & 0 & 0 & 0 & 0 & 0 & 0 & 0 & 0 & 0 & 0 \\
0 & 0 & 0 & 0 & 0 & 0 & 0 & B1 & 0 & 0 & 0 & 0 & 0 & B2 & 0 & 0 & B3 & B4 & 0 & 0 & 0 & 0 & 0 & B5 & 0 & 0 & B6 & B7 & 0 & 0 & B8 & B9 & B10 & 0 & 0 & 0 & 0 & 0 & 0 & 0 & 0 & 0 & 0 & 0 & 0 & 0 & 0 & 0 & 0 & 0 & 0 & 0 & 0 & 0 & 0 & 0 \\
0 & 0 & 0 & 0 & 0 & 0 & 0 & 0 & B1 & 0 & 0 & 0 & 0 & 0 & B2 & 0 & 0 & B3 & B4 & 0 & 0 & 0 & 0 & 0 & B5 & 0 & 0 & B6 & B7 & 0 & 0 & B8 & B9 & B10 & 0 & 0 & 0 & 0 & 0 & 0 & 0 & 0 & 0 & 0 & 0 & 0 & 0 & 0 & 0 & 0 & 0 & 0 & 0 & 0 & 0 & 0 \\
0 & 0 & 0 & 0 & 0 & 0 & 0 & 0 & 0 & B1 & 0 & 0 & 0 & 0 & 0 & B2 & 0 & 0 & B3 & B4 & 0 & 0 & 0 & 0 & 0 & B5 & 0 & 0 & B6 & B7 & 0 & 0 & B8 & B9 & B10 & 0 & 0 & 0 & 0 & 0 & 0 & 0 & 0 & 0 & 0 & 0 & 0 & 0 & 0 & 0 & 0 & 0 & 0 & 0 & 0 & 0 \\
0 & 0 & 0 & 0 & 0 & C1 & 0 & 0 & 0 & 0 & 0 & C2 & 0 & C3 & C4 & 0 & 0 & 0 & 0 & 0 & 0 & C5 & 0 & C6 & C7 & 0 & C8 & C9 & C10 & 0 & 0 & 0 & 0 & 0 & 0 & 0 & 0 & 0 & 0 & 0 & 0 & 0 & 0 & 0 & 0 & 0 & 0 & 0 & 0 & 0 & 0 & 0 & 0 & 0 & 0 & 0 \\
0 & 0 & 0 & 0 & 0 & 0 & C1 & 0 & 0 & 0 & 0 & 0 & C2 & 0 & C3 & C4 & 0 & 0 & 0 & 0 & 0 & 0 & C5 & 0 & C6 & C7 & 0 & C8 & C9 & C10 & 0 & 0 & 0 & 0 & 0 & 0 & 0 & 0 & 0 & 0 & 0 & 0 & 0 & 0 & 0 & 0 & 0 & 0 & 0 & 0 & 0 & 0 & 0 & 0 & 0 & 0 \\
0 & 0 & 0 & 0 & 0 & D1 & 0 & 0 & 0 & 0 & 0 & D2 & 0 & D3 & D4 & 0 & 0 & 0 & 0 & 0 & 0 & D5 & 0 & D6 & D7 & 0 & D8 & D9 & D10 & 0 & 0 & 0 & 0 & 0 & 0 & 0 & 0 & 0 & 0 & 0 & 0 & 0 & 0 & 0 & 0 & 0 & 0 & 0 & 0 & 0 & 0 & 0 & 0 & 0 & 0 & 0 \\
0 & 0 & 0 & 0 & 0 & 0 & D1 & 0 & 0 & 0 & 0 & 0 & D2 & 0 & D3 & D4 & 0 & 0 & 0 & 0 & 0 & 0 & D5 & 0 & D6 & D7 & 0 & D8 & D9 & D10 & 0 & 0 & 0 & 0 & 0 & 0 & 0 & 0 & 0 & 0 & 0 & 0 & 0 & 0 & 0 & 0 & 0 & 0 & 0 & 0 & 0 & 0 & 0 & 0 & 0 & 0 \\
0 & 0 & 0 & 0 & 0 & 0 & 0 & C1 & 0 & 0 & 0 & 0 & 0 & C2 & 0 & 0 & C3 & C4 & 0 & 0 & 0 & 0 & 0 & C5 & 0 & 0 & C6 & C7 & 0 & 0 & C8 & C9 & C10 & 0 & 0 & 0 & 0 & 0 & 0 & 0 & 0 & 0 & 0 & 0 & 0 & 0 & 0 & 0 & 0 & 0 & 0 & 0 & 0 & 0 & 0 & 0 \\
0 & 0 & 0 & 0 & 0 & 0 & 0 & 0 & C1 & 0 & 0 & 0 & 0 & 0 & C2 & 0 & 0 & C3 & C4 & 0 & 0 & 0 & 0 & 0 & C5 & 0 & 0 & C6 & C7 & 0 & 0 & C8 & C9 & C10 & 0 & 0 & 0 & 0 & 0 & 0 & 0 & 0 & 0 & 0 & 0 & 0 & 0 & 0 & 0 & 0 & 0 & 0 & 0 & 0 & 0 & 0 \\
0 & 0 & 0 & 0 & 0 & 0 & 0 & 0 & 0 & C1 & 0 & 0 & 0 & 0 & 0 & C2 & 0 & 0 & C3 & C4 & 0 & 0 & 0 & 0 & 0 & C5 & 0 & 0 & C6 & C7 & 0 & 0 & C8 & C9 & C10 & 0 & 0 & 0 & 0 & 0 & 0 & 0 & 0 & 0 & 0 & 0 & 0 & 0 & 0 & 0 & 0 & 0 & 0 & 0 & 0 & 0 \\
0 & 0 & 0 & 0 & 0 & 0 & 0 & 0 & D1 & 0 & 0 & 0 & 0 & 0 & D2 & 0 & 0 & D3 & D4 & 0 & 0 & 0 & 0 & 0 & D5 & 0 & 0 & D6 & D7 & 0 & 0 & D8 & D9 & D10 & 0 & 0 & 0 & 0 & 0 & 0 & 0 & 0 & 0 & 0 & 0 & 0 & 0 & 0 & 0 & 0 & 0 & 0 & 0 & 0 & 0 & 0 \\
0 & 0 & 0 & 0 & 0 & 0 & 0 & 0 & 0 & D1 & 0 & 0 & 0 & 0 & 0 & D2 & 0 & 0 & D3 & D4 & 0 & 0 & 0 & 0 & 0 & D5 & 0 & 0 & D6 & D7 & 0 & 0 & D8 & D9 & D10 & 0 & 0 & 0 & 0 & 0 & 0 & 0 & 0 & 0 & 0 & 0 & 0 & 0 & 0 & 0 & 0 & 0 & 0 & 0 & 0 & 0 \\
0 & 0 & 0 & 0 & 0 & 0 & 0 & 0 & 0 & 0 & B1 & 0 & 0 & 0 & 0 & 0 & 0 & 0 & 0 & 0 & B2 & B3 & B4 & 0 & 0 & 0 & 0 & 0 & 0 & 0 & 0 & 0 & 0 & 0 & 0 & B5 & B6 & B7 & B8 & B9 & B10 & 0 & 0 & 0 & 0 & 0 & 0 & 0 & 0 & 0 & 0 & 0 & 0 & 0 & 0 & 0 \\
0 & 0 & 0 & 0 & 0 & 0 & 0 & 0 & 0 & 0 & 0 & B1 & 0 & 0 & 0 & 0 & 0 & 0 & 0 & 0 & 0 & B2 & 0 & B3 & B4 & 0 & 0 & 0 & 0 & 0 & 0 & 0 & 0 & 0 & 0 & 0 & B5 & 0 & B6 & B7 & 0 & B8 & B9 & B10 & 0 & 0 & 0 & 0 & 0 & 0 & 0 & 0 & 0 & 0 & 0 & 0 \\
0 & 0 & 0 & 0 & 0 & 0 & 0 & 0 & 0 & 0 & 0 & 0 & B1 & 0 & 0 & 0 & 0 & 0 & 0 & 0 & 0 & 0 & B2 & 0 & B3 & B4 & 0 & 0 & 0 & 0 & 0 & 0 & 0 & 0 & 0 & 0 & 0 & B5 & 0 & B6 & B7 & 0 & B8 & B9 & B10 & 0 & 0 & 0 & 0 & 0 & 0 & 0 & 0 & 0 & 0 & 0 \\
0 & 0 & 0 & 0 & 0 & 0 & 0 & 0 & 0 & 0 & 0 & 0 & 0 & B1 & 0 & 0 & 0 & 0 & 0 & 0 & 0 & 0 & 0 & B2 & 0 & 0 & B3 & B4 & 0 & 0 & 0 & 0 & 0 & 0 & 0 & 0 & 0 & 0 & B5 & 0 & 0 & B6 & B7 & 0 & 0 & B8 & B9 & B10 & 0 & 0 & 0 & 0 & 0 & 0 & 0 & 0 \\
0 & 0 & 0 & 0 & 0 & 0 & 0 & 0 & 0 & 0 & 0 & 0 & 0 & 0 & B1 & 0 & 0 & 0 & 0 & 0 & 0 & 0 & 0 & 0 & B2 & 0 & 0 & B3 & B4 & 0 & 0 & 0 & 0 & 0 & 0 & 0 & 0 & 0 & 0 & B5 & 0 & 0 & B6 & B7 & 0 & 0 & B8 & B9 & B10 & 0 & 0 & 0 & 0 & 0 & 0 & 0 \\
0 & 0 & 0 & 0 & 0 & 0 & 0 & 0 & 0 & 0 & 0 & 0 & 0 & 0 & 0 & B1 & 0 & 0 & 0 & 0 & 0 & 0 & 0 & 0 & 0 & B2 & 0 & 0 & B3 & B4 & 0 & 0 & 0 & 0 & 0 & 0 & 0 & 0 & 0 & 0 & B5 & 0 & 0 & B6 & B7 & 0 & 0 & B8 & B9 & B10 & 0 & 0 & 0 & 0 & 0 & 0 \\
0 & 0 & 0 & 0 & 0 & 0 & 0 & 0 & 0 & 0 & 0 & 0 & 0 & 0 & 0 & 0 & B1 & 0 & 0 & 0 & 0 & 0 & 0 & 0 & 0 & 0 & B2 & 0 & 0 & 0 & B3 & B4 & 0 & 0 & 0 & 0 & 0 & 0 & 0 & 0 & 0 & B5 & 0 & 0 & 0 & B6 & B7 & 0 & 0 & 0 & B8 & B9 & B10 & 0 & 0 & 0 \\
0 & 0 & 0 & 0 & 0 & 0 & 0 & 0 & 0 & 0 & 0 & 0 & 0 & 0 & 0 & 0 & 0 & B1 & 0 & 0 & 0 & 0 & 0 & 0 & 0 & 0 & 0 & B2 & 0 & 0 & 0 & B3 & B4 & 0 & 0 & 0 & 0 & 0 & 0 & 0 & 0 & 0 & B5 & 0 & 0 & 0 & B6 & B7 & 0 & 0 & 0 & B8 & B9 & B10 & 0 & 0 \\
0 & 0 & 0 & 0 & 0 & 0 & 0 & 0 & 0 & 0 & 0 & 0 & 0 & 0 & 0 & 0 & 0 & 0 & B1 & 0 & 0 & 0 & 0 & 0 & 0 & 0 & 0 & 0 & B2 & 0 & 0 & 0 & B3 & B4 & 0 & 0 & 0 & 0 & 0 & 0 & 0 & 0 & 0 & B5 & 0 & 0 & 0 & B6 & B7 & 0 & 0 & 0 & B8 & B9 & B10 & 0 \\
0 & 0 & 0 & 0 & 0 & 0 & 0 & 0 & 0 & 0 & 0 & 0 & 0 & 0 & 0 & 0 & 0 & 0 & 0 & B1 & 0 & 0 & 0 & 0 & 0 & 0 & 0 & 0 & 0 & B2 & 0 & 0 & 0 & B3 & B4 & 0 & 0 & 0 & 0 & 0 & 0 & 0 & 0 & 0 & B5 & 0 & 0 & 0 & B6 & B7 & 0 & 0 & 0 & B8 & B9 & B10 \\
0 & 0 & 0 & 0 & 0 & 0 & 0 & 0 & 0 & 0 & 0 & 0 & 0 & C1 & 0 & 0 & 0 & 0 & 0 & 0 & 0 & 0 & 0 & C2 & 0 & 0 & C3 & C4 & 0 & 0 & 0 & 0 & 0 & 0 & 0 & 0 & 0 & 0 & C5 & 0 & 0 & C6 & C7 & 0 & 0 & C8 & C9 & C10 & 0 & 0 & 0 & 0 & 0 & 0 & 0 & 0 \\
0 & 0 & 0 & 0 & 0 & 0 & 0 & 0 & 0 & 0 & 0 & 0 & 0 & 0 & C1 & 0 & 0 & 0 & 0 & 0 & 0 & 0 & 0 & 0 & C2 & 0 & 0 & C3 & C4 & 0 & 0 & 0 & 0 & 0 & 0 & 0 & 0 & 0 & 0 & C5 & 0 & 0 & C6 & C7 & 0 & 0 & C8 & C9 & C10 & 0 & 0 & 0 & 0 & 0 & 0 & 0 \\
0 & 0 & 0 & 0 & 0 & 0 & 0 & 0 & 0 & 0 & 0 & 0 & 0 & 0 & 0 & C1 & 0 & 0 & 0 & 0 & 0 & 0 & 0 & 0 & 0 & C2 & 0 & 0 & C3 & C4 & 0 & 0 & 0 & 0 & 0 & 0 & 0 & 0 & 0 & 0 & C5 & 0 & 0 & C6 & C7 & 0 & 0 & C8 & C9 & C10 & 0 & 0 & 0 & 0 & 0 & 0 \\
0 & 0 & 0 & 0 & 0 & 0 & 0 & 0 & 0 & 0 & 0 & 0 & 0 & 0 & D1 & 0 & 0 & 0 & 0 & 0 & 0 & 0 & 0 & 0 & D2 & 0 & 0 & D3 & D4 & 0 & 0 & 0 & 0 & 0 & 0 & 0 & 0 & 0 & 0 & D5 & 0 & 0 & D6 & D7 & 0 & 0 & D8 & D9 & D10 & 0 & 0 & 0 & 0 & 0 & 0 & 0 \\
0 & 0 & 0 & 0 & 0 & 0 & 0 & 0 & 0 & 0 & 0 & 0 & 0 & 0 & 0 & D1 & 0 & 0 & 0 & 0 & 0 & 0 & 0 & 0 & 0 & D2 & 0 & 0 & D3 & D4 & 0 & 0 & 0 & 0 & 0 & 0 & 0 & 0 & 0 & 0 & D5 & 0 & 0 & D6 & D7 & 0 & 0 & D8 & D9 & D10 & 0 & 0 & 0 & 0 & 0 & 0 \\
0 & 0 & 0 & 0 & 0 & 0 & 0 & 0 & 0 & 0 & 0 & 0 & 0 & 0 & 0 & 0 & C1 & 0 & 0 & 0 & 0 & 0 & 0 & 0 & 0 & 0 & C2 & 0 & 0 & 0 & C3 & C4 & 0 & 0 & 0 & 0 & 0 & 0 & 0 & 0 & 0 & C5 & 0 & 0 & 0 & C6 & C7 & 0 & 0 & 0 & C8 & C9 & C10 & 0 & 0 & 0 \\
0 & 0 & 0 & 0 & 0 & 0 & 0 & 0 & 0 & 0 & 0 & 0 & 0 & 0 & 0 & 0 & 0 & C1 & 0 & 0 & 0 & 0 & 0 & 0 & 0 & 0 & 0 & C2 & 0 & 0 & 0 & C3 & C4 & 0 & 0 & 0 & 0 & 0 & 0 & 0 & 0 & 0 & C5 & 0 & 0 & 0 & C6 & C7 & 0 & 0 & 0 & C8 & C9 & C10 & 0 & 0 \\
0 & 0 & 0 & 0 & 0 & 0 & 0 & 0 & 0 & 0 & 0 & 0 & 0 & 0 & 0 & 0 & 0 & 0 & C1 & 0 & 0 & 0 & 0 & 0 & 0 & 0 & 0 & 0 & C2 & 0 & 0 & 0 & C3 & C4 & 0 & 0 & 0 & 0 & 0 & 0 & 0 & 0 & 0 & C5 & 0 & 0 & 0 & C6 & C7 & 0 & 0 & 0 & C8 & C9 & C10 & 0 \\
0 & 0 & 0 & 0 & 0 & 0 & 0 & 0 & 0 & 0 & 0 & 0 & 0 & 0 & 0 & 0 & 0 & 0 & 0 & C1 & 0 & 0 & 0 & 0 & 0 & 0 & 0 & 0 & 0 & C2 & 0 & 0 & 0 & C3 & C4 & 0 & 0 & 0 & 0 & 0 & 0 & 0 & 0 & 0 & C5 & 0 & 0 & 0 & C6 & C7 & 0 & 0 & 0 & C8 & C9 & C10 \\
0 & 0 & 0 & 0 & 0 & 0 & 0 & 0 & 0 & 0 & 0 & 0 & 0 & 0 & 0 & 0 & 0 & 0 & D1 & 0 & 0 & 0 & 0 & 0 & 0 & 0 & 0 & 0 & D2 & 0 & 0 & 0 & D3 & D4 & 0 & 0 & 0 & 0 & 0 & 0 & 0 & 0 & 0 & D5 & 0 & 0 & 0 & D6 & D7 & 0 & 0 & 0 & D8 & D9 & D10 & 0 \\
0 & 0 & 0 & 0 & 0 & 0 & 0 & 0 & 0 & 0 & 0 & 0 & 0 & 0 & 0 & 0 & 0 & 0 & 0 & D1 & 0 & 0 & 0 & 0 & 0 & 0 & 0 & 0 & 0 & D2 & 0 & 0 & 0 & D3 & D4 & 0 & 0 & 0 & 0 & 0 & 0 & 0 & 0 & 0 & D5 & 0 & 0 & 0 & D6 & D7 & 0 & 0 & 0 & D8 & D9 & D10
\end{matrix}
$$

Bibliography

1. S. Erwin, "Air Force: SSA is no more; its Space Domain Awareness," 2019. https://spacenews.com/air-force-ssa-is-no-more-its-space-domain-awareness/, Accessed January, 2020.

2. USSF, "United States Space Force," 2020. https://en.wikipedia.org/wiki/United_States_Space_Force, Accessed January, 2020.

3. UCS, "UCS Satellite Database: In-depth details on the 2,218 satellites currently orbiting Earth, including their country of origin, purpose, and other operational details," 2019. https://www.ucsusa.org/resources/satellite-database, Accessed January, 2020.

4. SpaceX, "Starlink Mission," 2019. https://www.spacex.com/webcast, Accessed December, 2019.

5. NASA, "Space Debris and Human Spacecraft." https://www.nasa.gov/mission_pages/station/news/orbital_debris.html, Accessed November, 2019.

6. NASA, "Observatories Across the Electromagnetic Spectrum," 2020. https://imagine.gsfc.nasa.gov/science/toolbox/emspectrum_observatories1.html, Accessed December, 2019.

7. W. Clohessy and R. Wiltshire, "Terminal Guidance System for Satellite Rendezvous," *Journal of the Aerospace Sciences*, pp. 653–658, 1960.

8. W. E. Wiesel, *Spaceflight Dynamics*. Aphelion Press, 3rd ed., 2010.

9. J. A. Hess, "Osculating Relative Orbit Elements Resulting from Chief Eccentricity and J2 Perturbing Forces," Master's thesis, Air Force Institute of Technology, 2011.

10. D. Barnes, "An Analysis of Radio-Frequency Geolocation Techniques for Satellite Systems Design," Master's thesis, Air Force Institute of Technology, 2017.

11. K. T. Alfriend, S. Vadali, P. Gurfil, J. P. How, and L. S. Breger, *Spacecraft Formation Flying: Dynamics, control and navigation*. Elsevier, 2010.

12. NOAA, "The Global Positioning System," 2017. `https://www.gps.gov/systems/gps/`, Accessed November, 2019.

13. NOAA and NASA, "GOES Mission Overview," 2020. `https://www.goes-r.gov/`, Accessed September, 2019.

14. ESA, "GRACE (Gravity Recovery And Climate Experiment)," 2019. `https://directory.eoportal.org/web/eoportal/satellite-missions/content/-/article/grace`, Accessed November, 2019.

15. B. Lieberman, "Orbital Inspectors," *Air Space Magazine*, 2014. `https://www.airspacemag.com/space/orbital-inspectors-180953376/`, Accessed November, 2019.

16. H. Schaub and J. Junkins, *Analytical Mechanics of Space Systems*. AIAA, 3rd ed., 2014.

17. D. Cajacob, N. Mccarthy, T. O'Shea, and R. McGwier, "Geolocation of RF Emitters with a Formation-Flying Cluster of Three Microsatellites," in *30th Annual AIAA/USU Conference on Small Satellites*, 2016.

18. F. Guo, Y. Fan, Y. Zhou, C. Zhou, and Q. Li, *Space Electronic Reconnaissance*. John Wiley & Sons, Singapore Pte. Ltd, 2014.

19. D. Vallado, *Fundamentals of Astrodynamics and Applications*. Hawthorne, CA: Microcosm Press: New York, NY: Springer, 2007.

20. D. K. Geller and A. Perez, "Initial Relative Orbit Determination for Close-in Proximity Operations," *Journal of Guidance, Control, and Dynamics*, vol. 38, no. 9, pp. 1833–1842, 2015.

21. E. Bailey, "Single Platform Geolocation of Radio Frequency Emitters," Master's thesis, Air Force Institute of Technology, 2015.

22. A. J. Sinclair, T. A. Lovell, and J. Darling, "RF localization solution using heterogeneous TDOA," in *IEEE Aerospace Conference Proceedings*, vol. 2015-June, IEEE Computer Society, jun 2015.

23. S. Shuster, A. J. Sinclair, and T. A. Lovell, "Initial relative-orbit determination using heterogeneous TDOA," in *2017 IEEE Aerospace Conference*, pp. 1–7, IEEE, mar 2017.

24. K. A. Legrand, K. J. Demars, and J. E. Darling, "Solutions of multivariate polynomial systems using macaulay resultant expressions," vol. 152, 2014.

25. D. Manocha, "Computing Selected Solutions of Polynomial Equations," 1994.

26. A. Morgan, *Solving Polynomial Systems Using Continuation for Engineering and Scientific Problems*. Society for Industiral and Applied Mathematics (SIAM), 2009.

27. J. A. Hess, *Adaptive Estimation and Heuristic Optimization of Nonlinear Spacecraft Attitude Dynamics*. PhD thesis, Air Force Institute of Technology, 2016.

28. R. Poli, "Analysis of the Publications on the Applications of Particle Swarm Optimisation," *Journal of Artificial Evolution and Applications*, vol. 2008, no. 2, pp. 1–10, 2008.

29. D. Lujan, T. A. Lovell, and T. Henderson, "Analysis of a Particle Swarm Optimizer of Space-Based Receivers for Geolocation Using Heterogeneous TDOA," 2019.

REPORT DOCUMENTATION PAGE

Form Approved
OMB No. 0704-0188

1. REPORT DATE *(DD-MM-YYYY)*	**2. REPORT TYPE**	**3. DATES COVERED** *(From - To)*
03/26/2020	Master's Thesis	Sept 2018 - Mar 2020

4. TITLE AND SUBTITLE
Space-Based Localization of Radio Frequency Transmitters Utilizing Macaulay Resultant and Heuristic Optimization Methods

5a. CONTRACT NUMBER

5b. GRANT NUMBER

5c. PROGRAM ELEMENT NUMBER

6. AUTHOR(S)
Wightman, Jessica, M, Capt

5d. PROJECT NUMBER
20Y356D

5e. TASK NUMBER

5f. WORK UNIT NUMBER

7. PERFORMING ORGANIZATION NAME(S) AND ADDRESS(ES)
Air Force Institute of Technology
Graduate School of Engineering and Management (AFIT/EN)
2950 Hobson Way
Wright-Patterson AFB OH 45433-7765

8. PERFORMING ORGANIZATION REPORT NUMBER
AFIT-ENY-MS-20-M-286

9. SPONSORING/MONITORING AGENCY NAME(S) AND ADDRESS(ES)
Air Force Research Labs, Space Vehicles Directorate
Dr. Alan Lovell, Dr. Andrew Sinclair
3550 Aberdeen Avenue SE
Kirtland AFB, NM 87117

10. SPONSOR/MONITOR'S ACRONYM(S)
AFRL/RV

11. SPONSOR/MONITOR'S REPORT NUMBER(S)

12. DISTRIBUTION/AVAILABILITY STATEMENT
Distribution Statement A. Approved for Public Release; Distribution is Unlimited

13. SUPPLEMENTARY NOTES
This work is declared a work of the U.S. Government and is not subject to copyright protection in the United States.

14. ABSTRACT
This research focuses on radio frequency geolocation of space objects utilizing space-based platforms. Geolocation has long been the solution for locating objects. In particular, this study examines the scenario of two cooperative receivers geolocating a transmitter in close proximity. An algorithm is developed to calculate the initial estimated transmitter location and projected orbital trajectory. The algorithm uses the Macaulay method of solving a system of polynomials as well as heuristic optimization techniques to locate a transmitter with respect to receivers at different time intervals. For the scenarios investigated, both Macaulay and heuristic optimization methods achieve initial relative orbit determination.

15. SUBJECT TERMS
relative satellite motion, polynomial systems, clohessy-wiltshire, rendezvous and proximity operations, initial relative orbit determination

16. SECURITY CLASSIFICATION OF:			**17. LIMITATION OF ABSTRACT**	**18. NUMBER OF PAGES**	**19a. NAME OF RESPONSIBLE PERSON**
a. REPORT	**b. ABSTRACT**	**c. THIS PAGE**			Maj Joshuah Hess, AFIT/ENY
					19b. TELEPHONE NUMBER *(Include area code)*
U	U	U	UU	79	(937) 255-3636 x4713